DOE/MC/11076-2788
(DE90000457)

Chemical Equilibria Model Analysis of Hope Creek Eastern Oil Shale Lysimeter Leachate Data

Topical Report

M.E. Essington

Work Performed Under Cooperative Agreement: DE-FC21-86MC11076

For
U.S. Department of Energy
Office of Fossil Energy
Morgantown Energy Technology Center
P.O. Box 880
Morgantown, West Virginia 26507-0880

By
Western Research Institute
P.O. Box 3395
University Station
Laramie, Wyoming 82071

September 1989

DOE/MC/11076--2788

DE90 000457

Chemical Equilibria Model Analysis of Hope Creek Eastern Oil Shale Lysimeter Leachate Data

Topical Report

M.E. Essington

September 1989

Work Performed Under Cooperative Agreement: DE-FC21-86MC11076

For
U.S. Department of Energy
Office of Fossil Energy
Morgantown Energy Technology Center
Morgantown, West Virginia

By
Western Research Institute
Laramie, Wyoming

DISCLAIMER

Available to DOE and DOE contractors from the Office of Scientific and Technical Information, P.O. Box 62, Oak Ridge, TN 37831; prices available from (615)576-8401, FTS 626-8401.

Available to the public from the National Technical Information Service, U.S. Department of Commerce, 5285 Port Royal Rd., Springfield, VA 22161.

Price: Printed copy AO4
Microfiche AO1

Codes are used for pricing all publications. The code is determined by the number of pages in the publication. Information pertaining to the pricing codes can be found in the current issues of the following publications, which are generally available in most libraries: *Energy Research Abstracts (ERA), Government Reports Announcements* and *Index (GRA* and *I); Scientific and Technical Abstracts Reports (STAR);* and publication NTIS-PR-360 available from NTIS at the above address.

TABLE OF CONTENTS

LIST OF TABLES

LIST OF FIGURES

SUMMARY

Leachates from field lysimeters containing an eastern oil shale, a retorted eastern oil shale, and an oil shale fines/retorted oil shale mixture were subjected to chemical equilibria analysis by the GEOCHEM model. Results of the chemical equilibria model analysis provided a more detailed characterization of the chemistry of oil shale materials. The aqueous chemistry of the lysimeter leachates is dominated by free ionic metal species and metal sulfate ion pairs. Activity diagrams show that free metal ion activities (with the exception of Ca^{2+}) are directly related to SO_4^{2-} activities. This suggests that the aqueous activities of the metals examined are not supported by metal sulfate solid phases. However, an examination of metal sulfate ion activity products (IAPs) as a function of time shows that the IAPs approach constant values after approximately 800 days of the field study. For the great majority of the metals examined, the IAP values suggest leachate undersaturation with respect to even the most stable metal sulfate phases. Leachates from all three materials are predicted by GEOCHEM to approach equilibrium with respect to gypsum ($CaSO_4 \cdot 2H_2O$) and goethite (FeOOH). In addition, leachates from the oil shale lysimeter are predicted by GEOCHEM to approach equilibrium with respect to melanterite ($FeSO_4 \cdot 7H_2O$), Fe-jurbanite ($FeSO_4OH$), franklinite ($ZnFe_2O_4$), molybdite (MoO_3), and molybdic acid (H_2MoO_4). Aluminum activities in all three lysimeter leachates fall within the stability region of several basic aluminum sulfates. However, Al^{3+} activities in the lysimeter leachates are not supported by sulfate phases.

INTRODUCTION

Recently, a five-year field lysimeter study designed to evaluate the reclamation and leachate generation characteristics of eastern oil shale material was completed. Leachates from the lysimeters were subjected to detailed chemical analyses, and the elemental release patterns were examined as a function of time. The objectives of the present study are to provide a more detailed characterization of the chemistry of lysimeter leachates by subjecting the leachate concentration data to chemical equilibria model analysis.

Background

The analysis of solid waste leachate data often includes the application of computer-based ion association models. These models, also termed chemical equilibria models, are based upon thermodynamic principles and use ion association constants, solubility product constants, and analytical concentration data to predict the distribution of an element between free anionic or cationic species, ion pairs and complexes, and solid phases. Although the ion association model has a firm theoretical basis, the computer codes used to perform the model calculations have a number of inherent shortcomings.

The more significant of these problems includes (1) an incomplete data set on solids controlling solution chemistry, their stoichiometry, crystallinity, and thermodynamic properties; (2) discrepancies in reported values for solubility and ion pair formation constants; (3) inability to thermodynamically describe various classes of reactions that influence leachate concentrations such as adsorption/desorption and ion exchange; (4) lack of thermodynamic data to characterize ion pair and complex ion formation reactions involving metal ions and organic ligands; (5) lack of accurate thermodynamic data for reduction-oxidation (redox) reactions; (6) variations in the thermodynamic data sets, both in the number of species considered and the associated data, used by the different chemical equilibria model computer codes; and (7) thermodynamic data are generally only available for standard conditions (298 K and 0.101 MPa). Such shortcomings cast doubt on the validity of model predictions, particularly when the models are applied to complex multicomponent systems such as spent oil shale. However, model predictions do provide a first approximation for understanding the complex chemistry of multicomponent systems.

Despite the shortcomings associated with chemical equilibria models, they have been extensively applied to provide useful insights into the chemistry of spent oil shale leachates. Saether and Runnells (1980) and Stollenwerk and Runnells (1981) used the thermodynamic models WATEQFC (Runnells and Lindburg 1981) and WATEQ2 (Truesdell and Jones 1974) to examine the solution chemistry of fluorine, molybdenum, and boron in spent oil shale leachates. They further used the model predictions to suggest the presence of fluorite (CaF_2) and powellite

($CaMoO_4$) in spent oil shale samples. Esmaili et al. (1985) used WATEQFC to characterize retorted oil shale aqueous extracts and to examine solubility relationships. Reddy and Lindsay (1986) examined the solubility relationships of calcium and magnesium minerals in spent oil shales using an ion association model. Similarly, Reddy et al. (1986) examined calcium and magnesium mineral solubility relationships and mineral transformations associated with spent oil shale recarbonation. Essington and Spackman (1986) used the PHREEQE (Parkhurst et al. 1980; Felmy et al. 1984) chemical equilibria model to elucidate the chemical status of spent oil shale leachates as a function of solid-solution contact time, temperature, solid to solution ratio, and carbon dioxide partial pressure. Essington et al. (1987) and Essington and Spackman (1988) used the GEOCHEM (Sposito and Mattigod 1980) chemical equilibria model to examine the solution and solid-phase chemistry of combusted eastern and western reference oil shale and recarbonated combusted western reference oil shale. Reddy et al. (1988a) used leachate data from weathering eastern (combusted and raw) oil shales and the WATEQFC model to elucidate the solubility relationships for zinc.

In additon to the generation of descriptive information on ion speciation and solubility relationships in spent oil shale leachates, chemical equilibria models have been used to predict element concentrations in spent oil shale leachates, generate thermodynamic data, identify attenuation mechanisms, and develop mineral weathering sequences. Essington and Spackman (1986) and Essington et al. (1987) observed that fluoride concentrations in spent oil shale leachates are controlled by the solubility of fluorite. Based on this information, Essington (1987) used the GEOCHEM code to predict the range of fluoride concentrations expected in retorted and combusted oil shale leachates. In general, the predicted range encompassed the measured values. Data generated from the application of the chemical equilibria models PHREEQE and GEOCHEM, using spent oil shale leachate data, have been used to generate the solubility product constant for powellite and the ion pair formation constants for $CaMoO_4^0$, $KMoO_4^-$, and $NaMoO_4^-$ (Essington in press). Spackman et al. (in press) used the GEOCHEM model to examine arsenate and selenite chemistry in retorted oil shales and distinguish between the attenuation mechanisms of adsorption and precipitation. Sullivan et al. (1988a and b) applied the WATEQFC model using leachate data from weathering eastern and combusted eastern oil shales. From the model predictions, they developed a weathering scheme that identified the secondary mineral forms of aluminum and iron and the chemical mechanisms for the production of acidity.

A great majority of studies that have used chemical equilibria models to characterize spent oil shale aqueous chemistry have been conducted under well-defined laboratory conditions. These studies include the characterization of equilibrium column leachates (Saether and Runnells 1980; Stollenwerk and Runnells 1981), the characterization of equilibrium aqueous extracts as a function of several experimental variables such as temperature, solid-to-solution ratio, carbon dioxide partial pressure, and reaction time (Essington and Spackman 1986, 1988;

Reddy and Lindsay 1986; Reddy et al. 1986; Essington et al. 1987; Reddy et al. 1988b), and the characterization of aqueous extracts from equilibrium and nonequilibrium laboratory simulated weathering studies (Reddy et al. 1988a; Sullivan et al. 1988a and b). Yet, the chemical equilibria model evaluation of leachates from field spent oil shale disposal sites has not been conducted.

Recently, a five-year field lysimeter study designed to evaluate the leaching characteristics of eastern oil shale and retorted eastern oil shale was completed (Robl 1989). Over 3800 leachate samples were collected and subjected to chemical analysis over the course of the study. Data evaluation included an analysis of element concentration and leachate pH changes with time as influenced by waste type. Limited chemical equilibria model analyses were also performed and the results used to suggest mechanisms controlling leachate chemical composition and acid generation. However, these evaluations were not detailed in scope.

Objective

The objective of the present study is to provide a more detailed characterization of the chemistry of leachates from eastern oil shale materials by subjecting the leachate concentration data from the lysimeter study to chemical equilibria model analysis.

METHODOLOGY

The Hope Creek eastern oil shale field lysimeter study was initiated in 1983 and completed in 1988. The study was designed to evaluate the environmental and reclamation characteristics of eastern oil shale and retorted eastern oil shale. The overall study objectives, lysimeter construction, raw and retorted eastern oil shale and associated materials (overburden and soil), emplacement configuration, sampling depths and frequency, and leaching results are reported elsewhere (Koppenaal et al. 1984; Robl et al. 1985, 1986, 1987, 1988; Robl 1989). The oil shale used in the study was mined from the Sunbury Shale and the Cleveland Member of the Ohio Shale and processed using the Dravo traveling grate retort. Overburden material was mined from the Nancy Member of the Borden Formation. The soil used in the study was from the Gilpin soil series.

Although eight lysimeters were constructed to simulate eight solid waste emplacement configurations, only three lysimeters were chosen for treatment by a chemical equilibria model. The emplacement designs for the three lysimeters were similar, the only significant difference being the type of waste material examined. Thus, the leachate chemistry of one waste type could be directly compared to that of another waste type. Lysimeter L3 contained a six-foot depth of a retorted oil shale/oil shale fines mixture overlaid with two feet of overburden material and a surface two feet of soil. Lysimeter L6 contained a six-foot depth of retorted oil shale with a surface cover identical to that of L3. Lysimeter L7 contained a six-foot depth of oil shale fines overlaid with three feet of overburden material and a surface foot of soil.

Leachates for model analysis were collected from sampling ports located at a depth of 10 feet (bottom of the lysimeter). Leachates examined in the present study are designated L310, L610, and L710 to identify lysimeter and leachate sampling depth. Each lysimeter contained three sampling ports at the 10-foot depth: left, center, and right ports. Model analysis was conducted on 20 samples (for which complete chemical analysis data were available) from each port for a total of 60 analyses per lysimeter. Leachate samples chosen for model analysis, as well as the chemical composition of the leachates, are tabulated in Appendix A.

The chemical analyses of lysimeter leachates were treated with the chemical equilibria model GEOCHEM. The model calculates the free ionic and ion pair species distribution of the leachate components by numerically solving a set of coupled nonlinear algebraic equations by successive iterations. Each mass-balance equation relates total soluble element concentration to free ionic and ion pair species concentrations using appropriate stability constants and stioichiomery. The equations are iterated numerically until a constant effective ionic strength for the solution is obtained. Conversion of GEOCHEM's thermodynamic data for use in the mass-balance equations and conversion of species concentrations to activities requires activity coefficients. Single-ion activity coefficients for charged species are calculated using the Davies equation. Single-ion activity coefficients for neutral species are calculated using the Setchenow-Harner-Owen equation with k_m equal to 0.1.

Lysimeter leachate chemical components considered in the chemical modeling are: pH, pe, Ca, Mg, K, Na, Fe(II), Fe(III), Mn, Cu, Cd, Zn, Ni, Pb, Al, SO_4, $B(OH)_4$, and MoO_4. Chemical analyses were also performed to determine total organic carbon (TOC), Cr, As, Se, NH_4, NO_3, Cl, and PO_4 concentrations in leachates. However, these were not considered in the model analysis because there was insufficient characterization for modeling purposes, insufficient modeling capabilities, or the concentrations were consistently below detectable concentrations. Species considered by the model, as well as associated stability constants are tabulated in Appendix B. The model predictions that are of greatest interest are the predicted free ionic activities. For the components listed above, excluding pe, these are H^+, Ca^{2+}, Mg^{2+}, K^+, Na^+, Fe^{2+}, Fe^{3+}, Mn^{2+}, Cu^{2+}, Cd^{2+}, Zn^{2+}, Ni^{2+}, Pb^{2+}, Al^{3+}, SO_4^{2-}, $B(OH)_4^-$, and MoO_4^{2-}. The free ionic activities will be used in the construction of activity diagrams to examine solubility relationships. Model predictions of secondary interest are the aqueous distributions of the components between free and ion pair species.

A number of assumptions are made in the application of GEOCHEM to the lysimeter leachate data. Calculation of the distribution of total Fe between Fe(II) and Fe(III) in each solution requires a value for the redox potential (pe). Because this parameter was not measured, estimation of pe for each solution is required. For the model evaluations, a moderately reducing pH + pe value of 9.0 was chosen. Thus, pe for each solution was calculated by subracting solution pH from 9.0. Results of a sensitivity analysis of the predicted Fe^{2+}/Fe^{3+} distribution to pe are listed in Table 1. Solution data for this evaluation were taken from lysimeter L610. These results show that Fe^{2+} dominates the Fe^{2+}/Fe^{3+} couple. Further, Fe^{2+} activity is invarient over a wide range of pe values, and predicted Fe^{3+} activities are directly correlated to assumed pe values. Thus, conclusions based on the predicted activities of Fe^{3+} must be interpreted cautiously.

Table 1. The Influence of pe on the $(Fe^{2+})/(Fe^{3+})$ Distribution

pe	$-\log(Fe^{2+})$	$-\log(Fe^{3+})$
NC[a]	3.02	--
4.0	3.02	11.83
5.0	3.02	10.83
6.0	3.02	9.83
7.0	3.02	8.83

[a] Fe_T is assumed to exist only in the Fe(II) oxidation state (the redox reaction $Fe^{2+} = Fe^{3+} + e^-$ is not considered).

Total organic carbon data were also compiled over the duration of the lysimeter studies. However, this information was not used in the model evaluations because GEOCHEM requires input for specific components. Because this is not available, the next option is to model the functional group composition of the organic carbon using several simple organic compounds (Mattigod and Sposito 1979). However, this requires knowledge of the types and relative proportions of organic functional groups present. Because such information is not available for the lysimeter leachates, inorganic-organic interactions were not considered by GEOCHEM. It is well known that soluble organics can significantly influence solution chemistry, specifically, the distribution of trace metal cations between free ionic and complexed species. Because organic ligands were not considered in the model evaluations the model predictions must be interpreted cautiously.

Finally, GEOCHEM calculations assume that the modeled systems are at 298 K. Clearly, this condition is not met in field studies. However, the absence of this condition does not diminish the value of the model results, particularly if they are used as a first approximation of the complex chemistry of leachates from processed oil shale solid wastes.

RESULTS AND DISCUSSION

Solution Speciation

The predicted aqueous speciation of elements in a leachate will be a function of the chemical composition of the leachate, the number of aqueous species considered in the model computations, and the magnitude of the stability constants that describe ion pair or complex ion formation. Because the anion chemistry of the lysimeter leachates is dominated by sulfate, cationic constituents are predicted to distribute between free ionic species and sulfate ion pairs. The sulfate ion pairs that dominate are of the form MSO_4^{m-2}, where M is the metal cation with m+ valence. Additionally, higher order sulfate ion pairs such as $M(SO_4)_2^{m-4}$ and $M(SO_4)_3^{m-6}$ are significant when M is Cd or Pb.

Figure 1 illustrates the percentage of total metal cation occurring as the free ionic species for the metals included for GEOCHEM analysis. Calcium and Na distributions (not illustrated) are similar to those depicted by Mg and K, respectively. Further, the Fe(II)/Fe(III) couple is dominated by Fe(II)(see Table 1). Thus, only the distribution of Fe(II) is illustrated in Figure 1.

In general, the percentage of any given metal occurring as the free cation is not highly variable as a function of time in lysimeter L310 and L610 leachates. Similarly, metals in L710 leachates, collected after approximately 600 days of study, show similar free-cation distributions to those predicted for L310 and L610 leachates. For the L710 leachates collected in the first 600 days of the study, the percentage of free metal increases with time from an initial minimum. Initially low free-metal percentages (high percentages of metal-sulfate ion pairs) that increase with time in lysimeter L710 leachates are a result of initially high sulfate concentrations that decrease with time.

The predicted aqueous distribution of molybdenum is illustrated in Figure 2. Leachates from lysimeter L310 are dominated by $HMoO_4^-$, $H_2MoO_4^0$, and $MgMoO_4^0$. Molybdate distributions in L610 and L710 leachates were dominated by $HMoO_4^-$ and $H_2MoO_4^0$ with lesser amounts of the $MgMoO_4^0$, MoO_4^{2-}, $CaMoO_4^0$, and $NaMoO_4^-$ species, respectively. Boron is predicted to exist as $B(OH)_3^0$ in all leachates examined (not illustrated). Further boron speciation into $M_a[B(OH)_3]_b^{am+}$ ion pairs was not predicted due to the limitations in the GEOCHEM thermodynamic data.

Solubility Relationships

The GEOCHEM calculated metal and ligand activities are used to construct solubility diagrams. These diagrams are used to define the chemical status (saturated, undersaturated, supersaturated) of the lysimeter leachates with respect to solids that may potentially occur in the oil shale materials. The dissolution of the solid $M_aL_b(s)$ in contact with an aqueous solution can be described by the reaction:

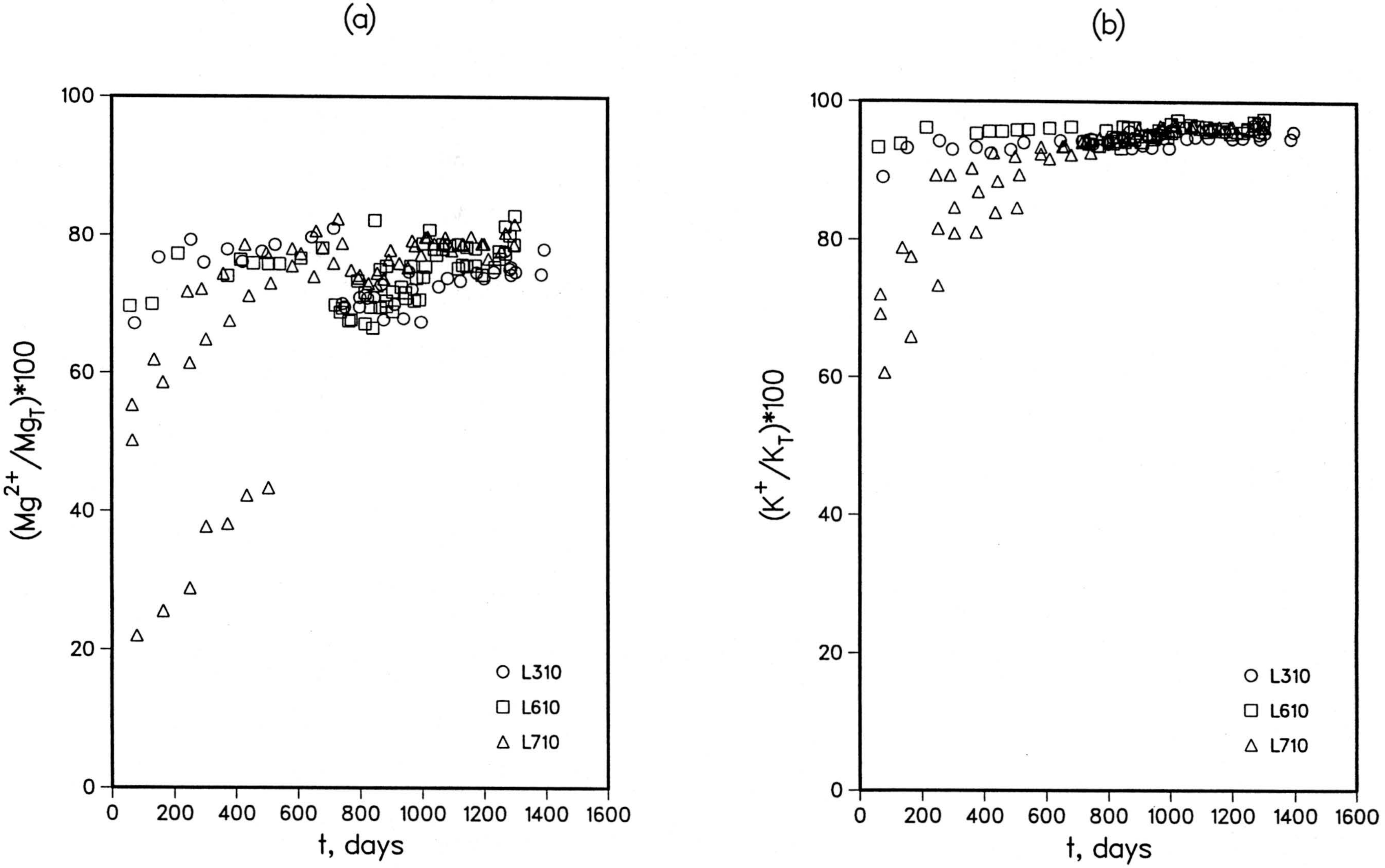

Figure 1. Percentage of Total Metal Occurring as the Free Ionic Species (a) Mg and (b) K.

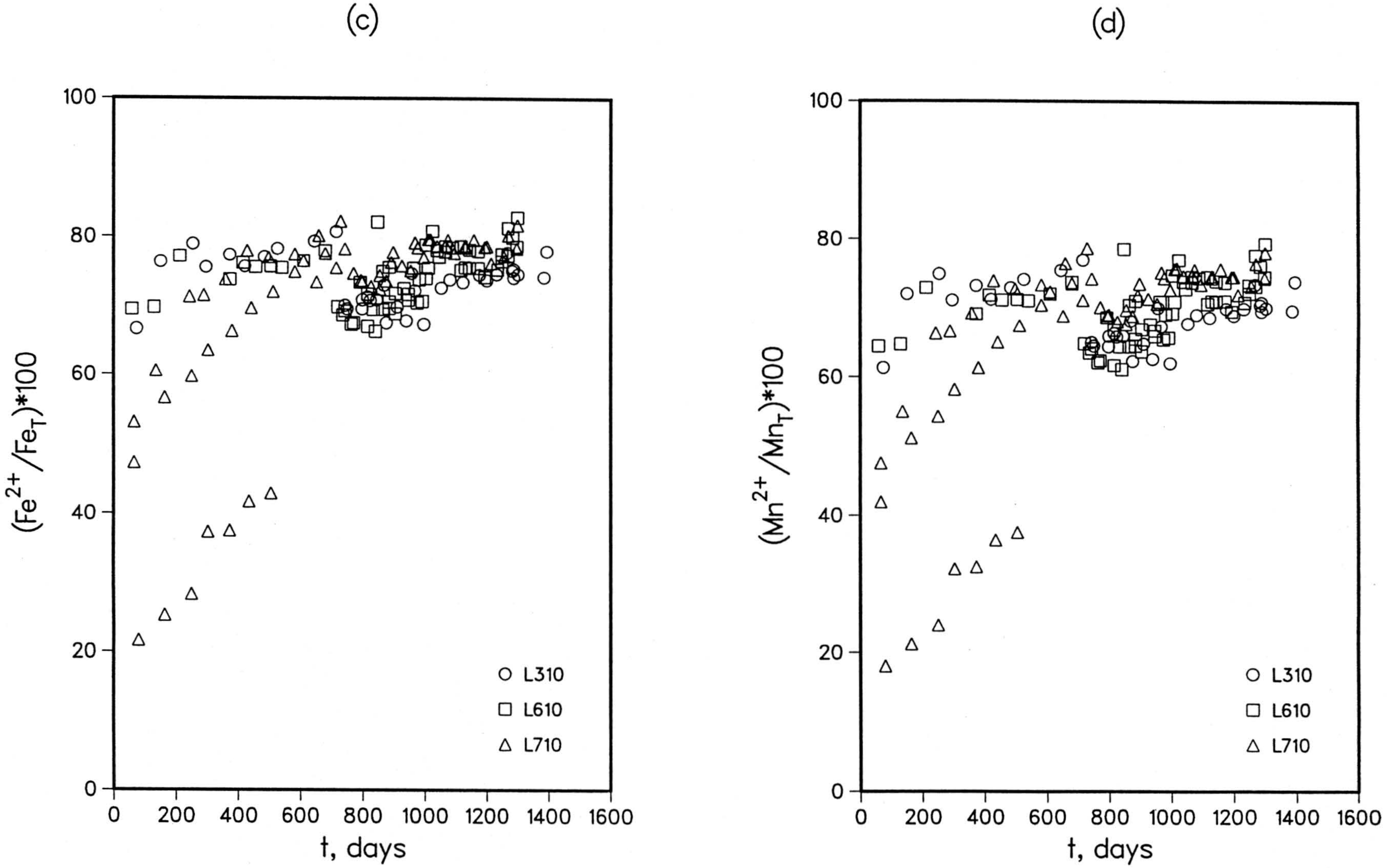

Figure 1 continued. Percentage of Total Metal Occurring as the Free Ionic Species (c) Fe and (d) Mn.

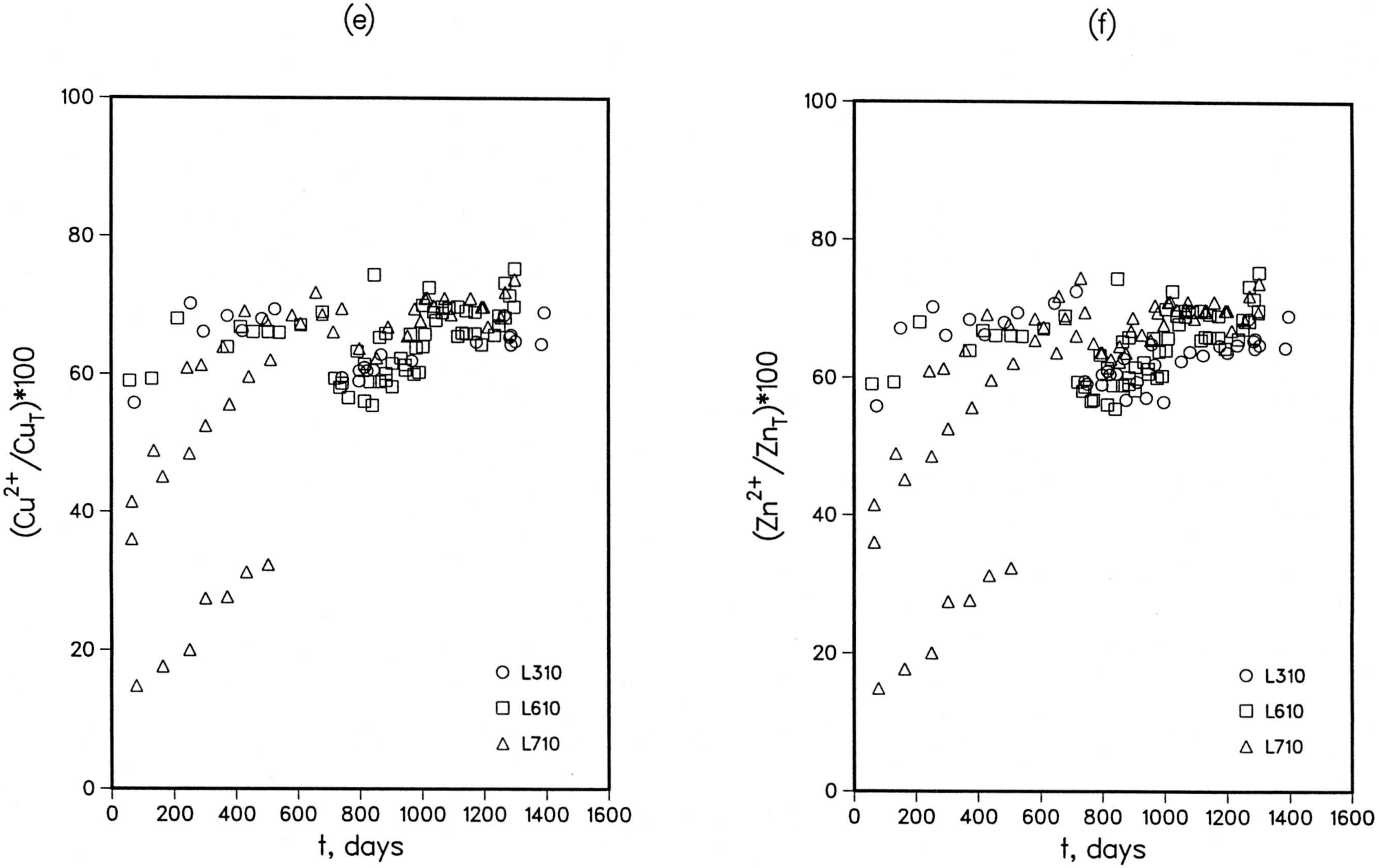

Figure 1 continued. Percentage of Total Metal Occurring as the Free Ionic Species (e) Cu and (f) Zn.

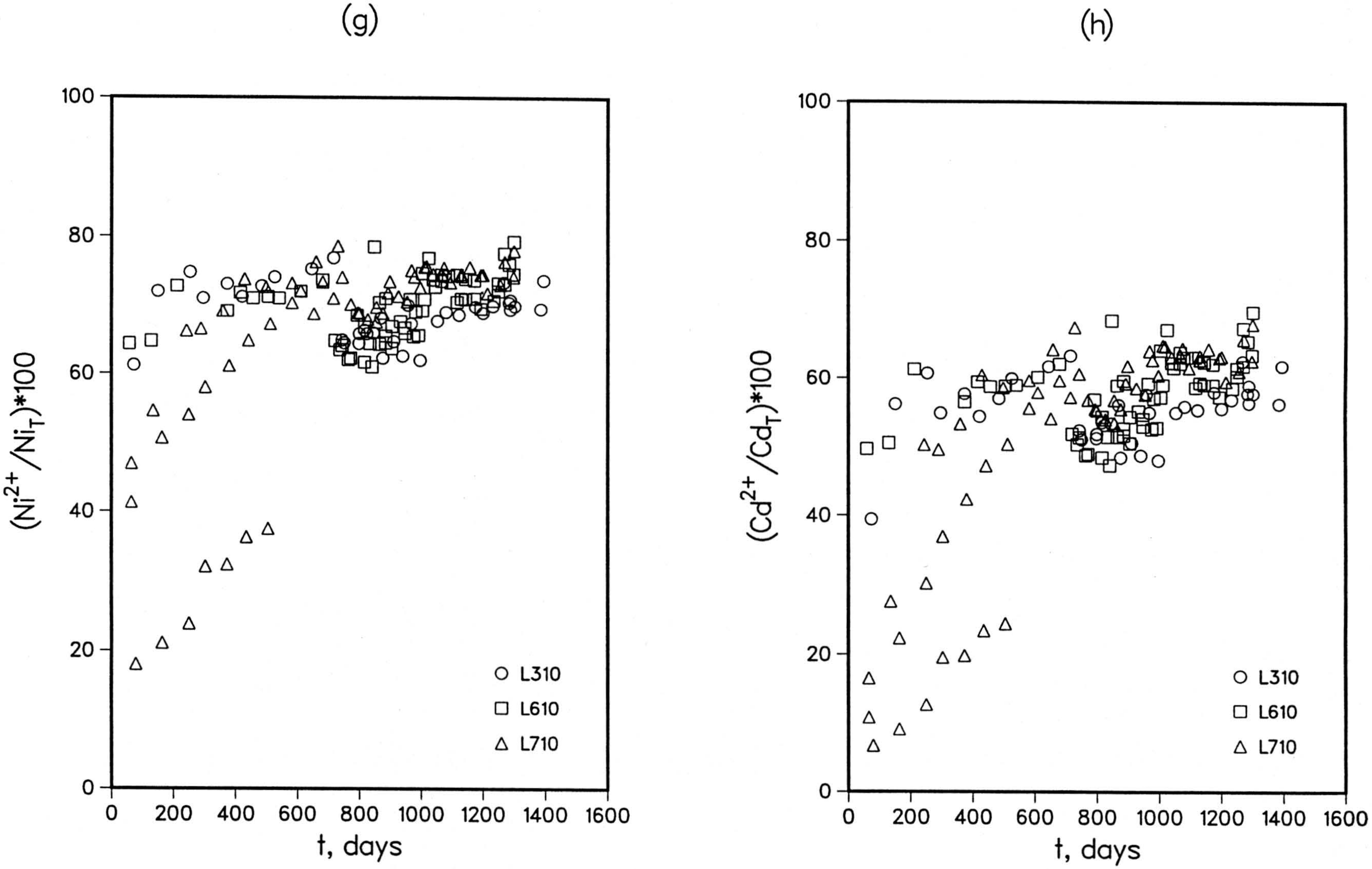

Figure 1 continued. Percentage of Total Metal Occurring as the Free Ionic Species (g) Ni and (h) Cd.

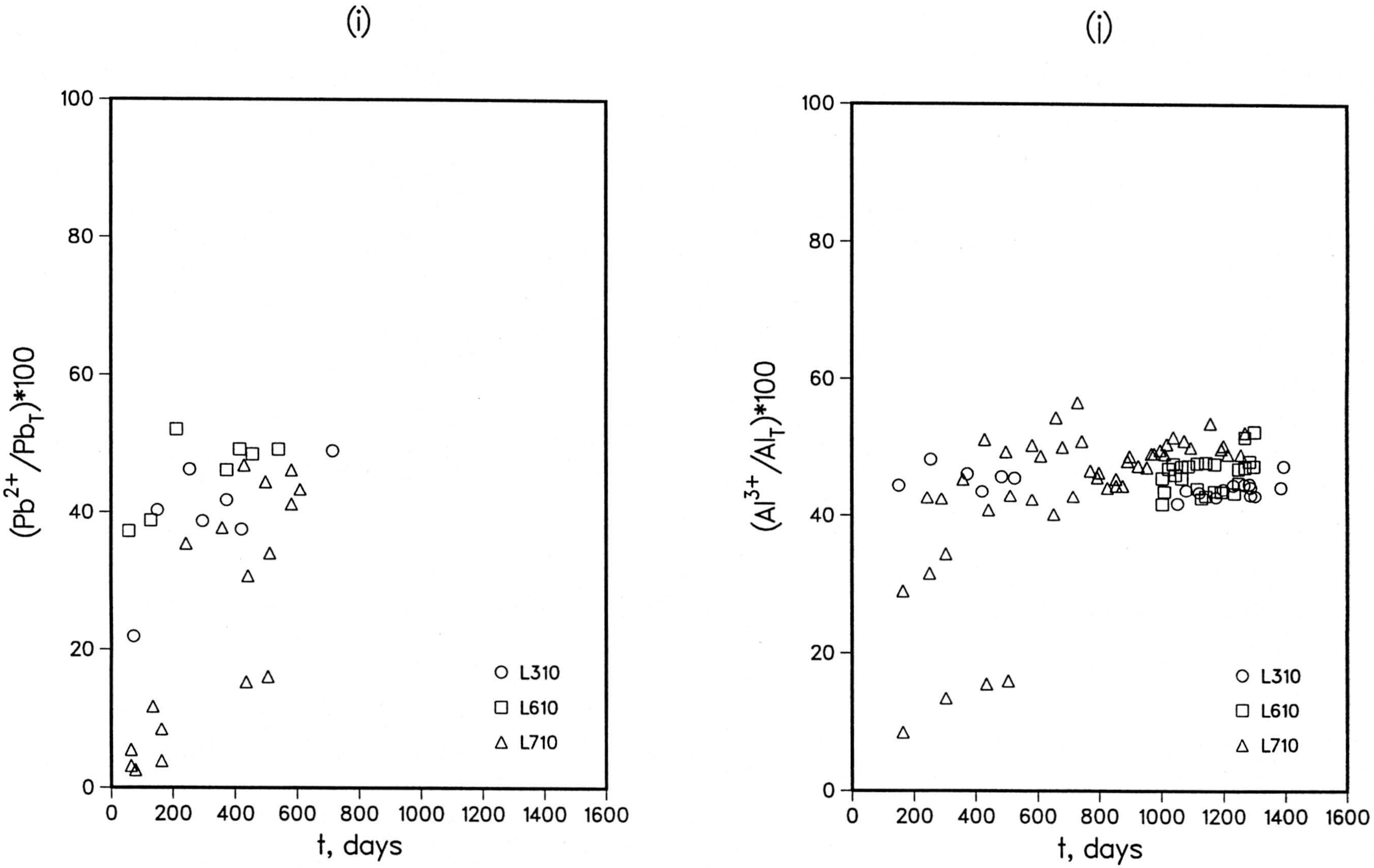

Figure 1 continued. Percentage of Total Metal Occurring as the Free Ionic Species (i) Pb and (j) Al.

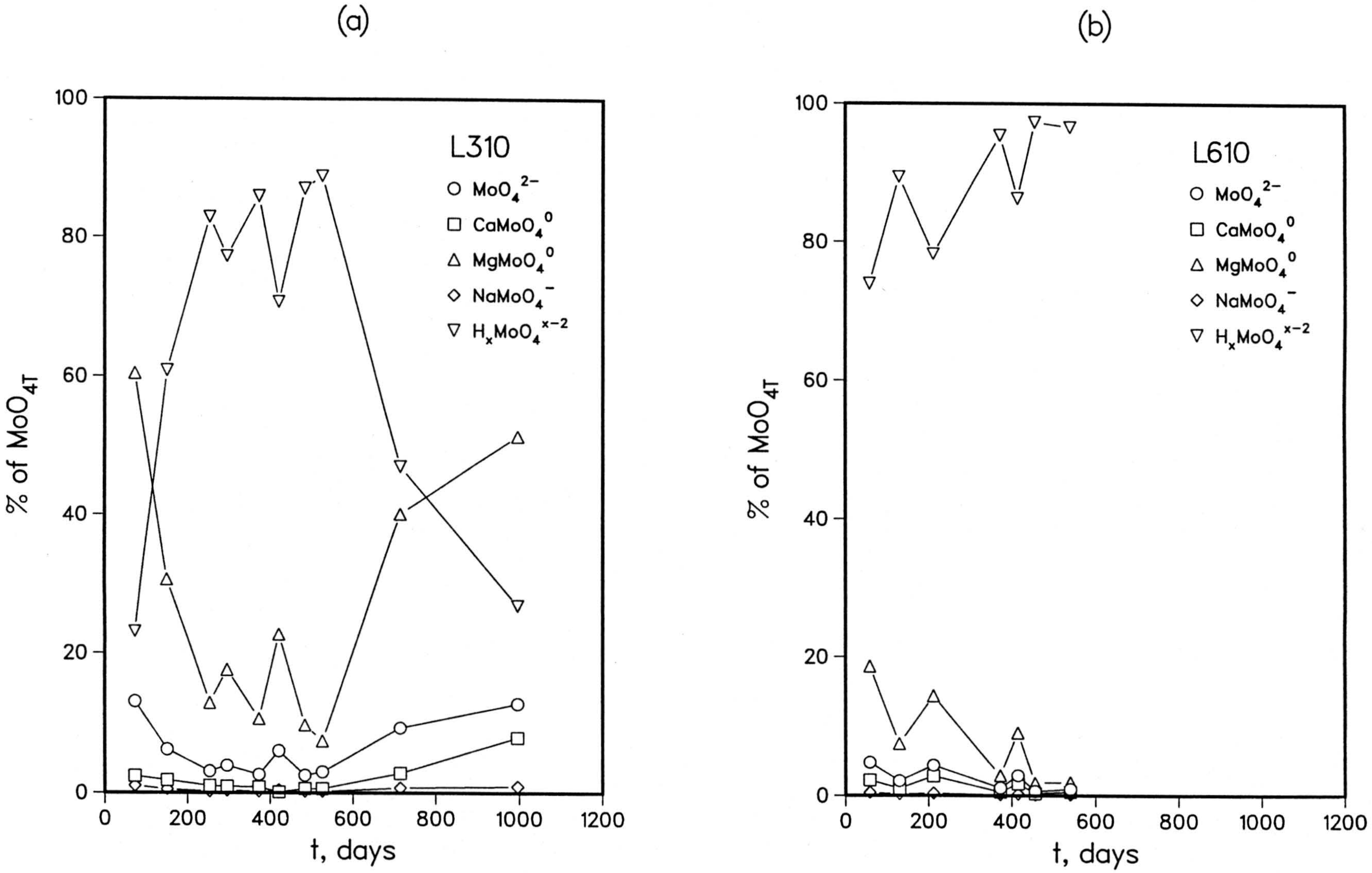

Figure 2. Aqueous Molybdenum Speciation in (a) L310, and (b) L610

(c)

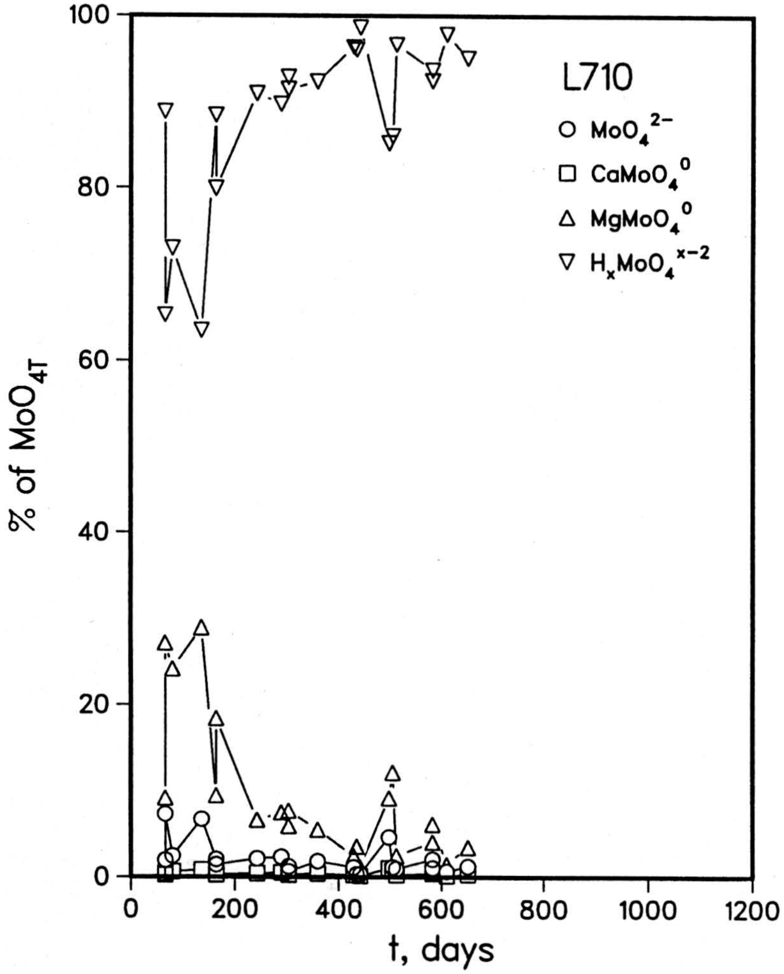

Figure 2 continued. Aqueous Molybdenum Speciation in (c) L710.

$$M_aL_b(s) = aM^{m+}(aq) + bL^{l-}(aq) \qquad (1)$$

where M is a metal ion with charge m+, L is a ligand ion with charge l-, and a and b are stoichiometric coefficients subject to the electroneutrality condition am = bl. For the reaction in equation 1 at equilibrium, the equilibrium solubility product constant, K_{sp}, is defined as:

$$K_{sp} = (M^{m+})^a(L^{l-})^b \qquad (2)$$

where parentheses signify the thermodynamic activity of the species enclosed.

A log transformation of equation 2 and rearrangement yields:

$$pK_{sp}/b - (a/b)pM^{m+} = pL^{l-} \qquad (3)$$

where p designates -log. Thus, the stability line for solid $M_aL_b(s)$ plotted on a pM^{m+} versus pL^{l-} graph will have a -a/b slope and a pK_{sp}/b intercept. The predicted metal and ligand activities, when plotted on such a diagram, shows the chemical status of a solution with respect to solid $M_aL_b(s)$. Data points that plot on the stability line suggest that the solution is saturated with respect to $M_aL_b(s)$. This is generally indirect evidence that the solid may be present and may be controlling the concentrations of M or L, assuming that equilibrium conditions prevail. If the predicted activity data do not plot on the stability line, then one of two conditions may exist: solution undersaturation or supersaturation with respect to $M_aL_b(s)$. Both conditions suggest that solution chemistry is not controlled by the particular solid. An undersaturated condition suggests that there is a potential for $M_aL_b(s)$ to dissolve, if it is present or added to the system. Further, a supersaturated condition merely suggests that there is a potential for $M_aL_b(s)$ to precipitate.

The GEOCHEM predicted activity data can also be used to examine solubility equilibria as a function of time by plotting the ion activity product (IAP) as a function of sampling time. Ion activity product values are a property of the solution and are calculated for specific mineral phases using the predicted ion activities. For example, the IAP for solid $M_aL_b(s)$ has the form:

$$IAP = (M^{m+})^a(L^{l-})^b \qquad (4)$$

If the calculated IAP is numerically equal to K_{sp}, then GEOCHEM predicts that the solution is controlled by the solid $M_aL_b(s)$. Ion activity product values greater than K_{sp} suggest solution supersaturation and IAP values less than K_{sp} suggest undersaturation. Solubility relationships used in this study are listed in Table 2.

The dominant anionic component of the lysimeter leachates is SO_4^{2-}. Thus, a great majority of the constructed solubility diagrams relate free-metal ion activity to SO_4^{2-} activity and, correspondingly,

Table 2. Solubility Relationships Used in this Study

Reaction	pK_{sp}	Source
Gypsum		
$CaSO_4 \cdot 2H_2O = Ca^{2+} + SO_4^{2-} + 2H_2O$	4.64	1
Epsomite		
$MgSO_4 \cdot 7H_2O = Mg^{2+} + SO_4^{2-} + 7H_2O$	2.14	2
Melanterite		
$FeSO_4 \cdot 7H_2O = Fe^{2+} + SO_4^{2-} + 7H_2O$	4.66	3
Goethite		
$FeOOH + 3H^+ = Fe^{3+} + 2H_2O$	0.02	4
K-jarosite		
$KFe_3(SO_4)_2(OH)_6 + 6H^+ = K^+ + 3Fe^{3+} + 2SO_4^{2-} + 6H_2O$	14.8	2
Na-jarosite		
$NaFe_3(SO_4)_2(OH)_6 + 6H^+ = Na^+ + Fe^{3+} + 2SO_4^{2-} + 6H_2O$	11.2	2
Fe-jurbanite		
$FeSO_4OH + H^+ = Fe^{3+} + SO_4^{2-} + H_2O$	10.06	5
Manganese Sulfate		
$MnSO_4 \cdot H_2O = Mn^{2+} + SO_4^{2-} + H_2O$	-0.47	4
Cupric Sulfate		
$CuSO_4 \cdot H_2O = Cu^{2+} + SO_4^{2-} + H_2O$	2.61	4
Cadmium Sulfate		
$CdSO_4 \cdot 8/3H_2O = Cd^{2+} + SO_4^{2-} + 8/3H_2O$	1.87	2
Goslarite		
$ZnSO_4 \cdot 7H_2O = Zn^{2+} + SO_4^{2-} + 7H_2O$	1.96	2
Franklinite		
$ZnFe_2O_4 + 8H^+ = Zn^{2+} + 2Fe^{3+} + 4H_2O$	-6.87	6
Morenosite		
$NiSO_4 \cdot 7H_2O = Ni^{2+} + SO_4^{2-} + 7H_2O$	2.36	2
Trevorite		
$NiFe_2O_4 + 8H^+ = Ni^{2+} + Fe^{3+} + 4H_2O$	-10.63	7

Table 2. Solubility Relationships Used in this Study (continued)

Reaction	pK_{sp}	Source
Gibbsite $Al(OH)_3 + 3H^+ = Al^{3+} + 3H_2O$	-8.77	2
Jurbanite $AlSO_4OH + H^+ = Al^{3+} + SO_4^{2-} + H_2O$	3.8	8
Basaluminite $Al_4SO_4(OH)_{10} + 10H^+ = 4Al^{3+} + SO_4^{2-} + 10H_2O$	-22.4	9
Alunite $KAl_3(SO_4)_2(OH)_6 + 6H^+ = K^+ + 3Al^{3+} + 2SO_4^{2-} + 6H_2O$	1.4	9
Molybdite $MoO_3 + H_2O = MoO_4^{2-} + 2H^+$	12.05	10
Molydbic Acid $H_2MoO_4(c) = MoO_4^{2-} + 2H^+$	13.34	10
Powellite $CaMoO_4 = Ca^{2+} + MoO_4^{2-}$	8.05	11

Source: (1) Reddy et al. (1988b), (2) Ball et al. (1980), (3) Runnells and Lindberg (1981), (4) Lindsay (1979), (5) Sullivan et al. (1988b), (6) Reddy et al. (1988a), (7) Naumov et al. (1974), (8) Nordstrom (1982), (9) Adams and Rawajfih (1977), (10) Reddy and Drever (1987), (11) Essington (1989).

allow metal sulfate solubility equilibria to be evaluated. Figure 3 illustrates the calcium sulfate equilibria for the lysimeter leachates. The activities of Ca^{2+} are inversely related to those of SO_4^{2-}. During the early stages of the study, all leachates are predicted to be supersaturated with respect to gypsum. However, after approximately 800 days of study, gypsum IAP values stabilize at a value slightly greater than the K_{sp}, suggesting supersaturated conditions. However, due to the assumptions used in the model analysis and the inherent uncertainties in the thermodynamic data, a calculated pIAP within ±0.5 of pK_{sp} is not an unreasonable definition of saturation. Thus, the lysimeter leachates are predicted by GEOCHEM to approach saturation with respect to gypsum. A similar conclusion was reached by Robl (1989) using the WATEQ code.

The activities of Mg^{2+} are directly related to SO_4^{2-} activities in leachates from all three lysimeters (Figure 4). This observation

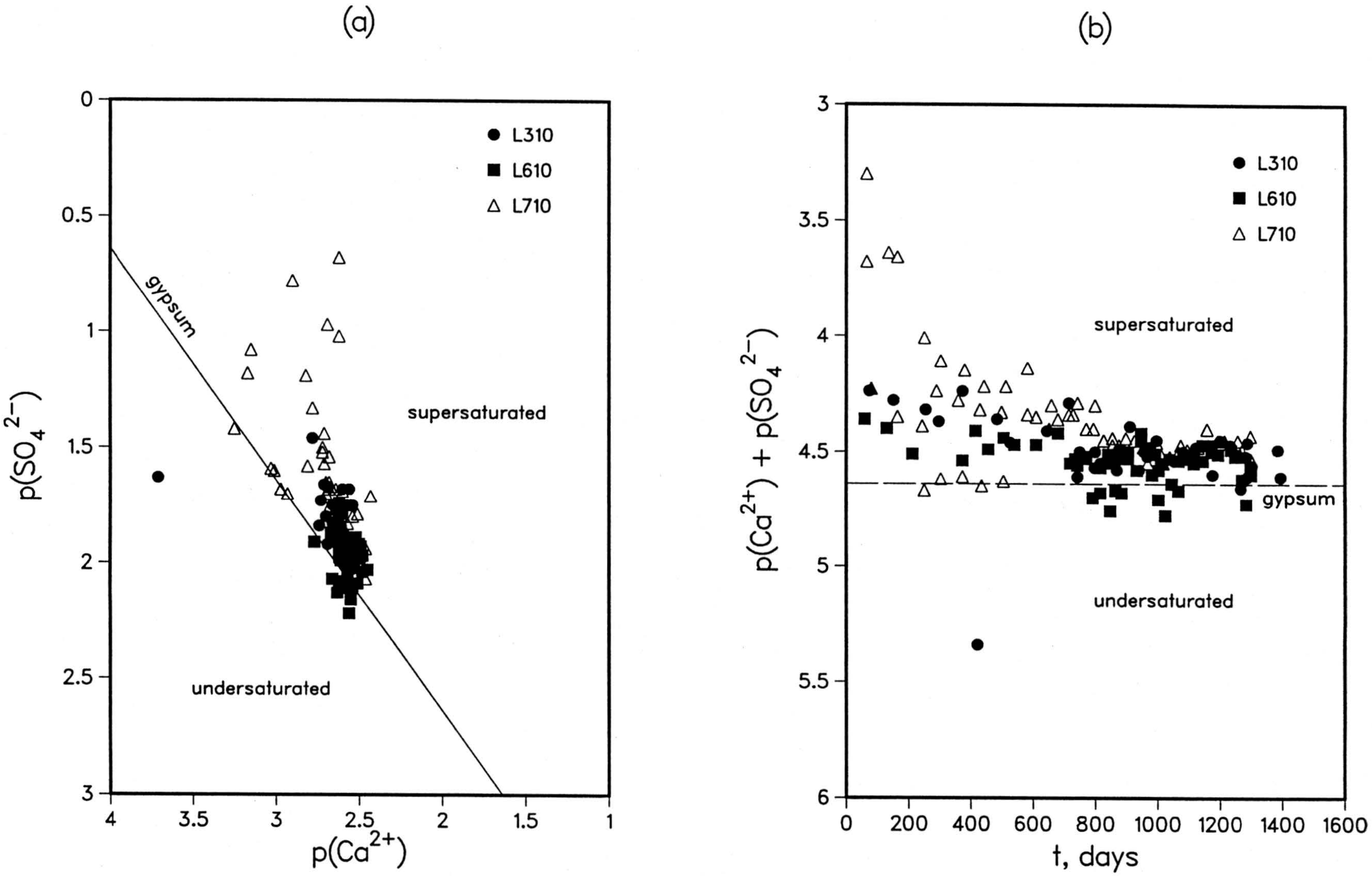

Figure 3. Calcium Sulfate Equilibria in Lysimeter Leachates

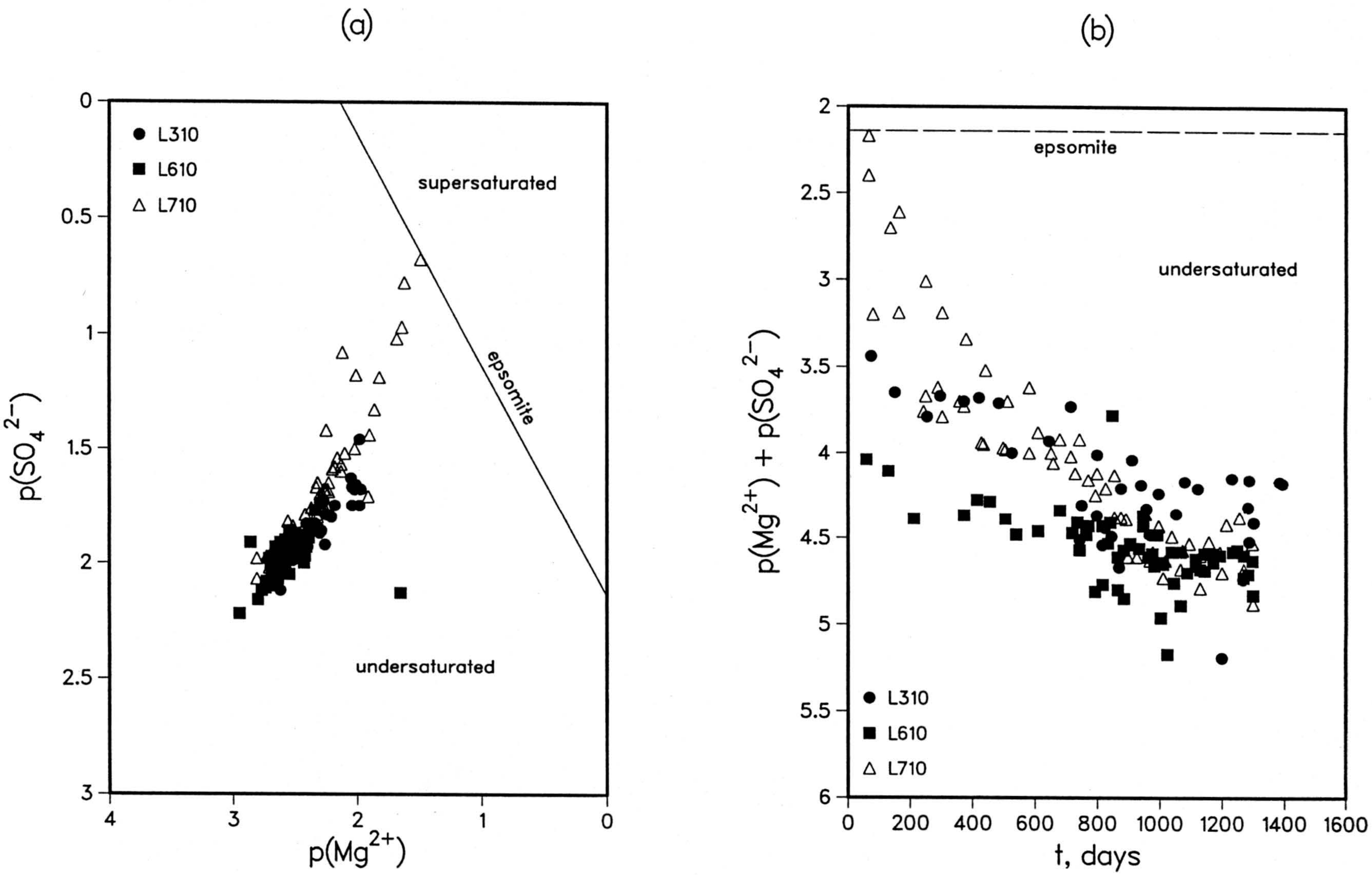

Figure 4. Magnesium Sulfate Equilibria in Lysimeter Leachates

corresponds to the element release patterns of the two elements and suggests that a magnesium sulfate is not influencing leachate chemistry. Further, the leachates are undersaturated with respect to epsomite ($MgSO_4 \cdot 7H_2O$), a relatively stable magnesium sulfate solid. Examination of the magnesium sulfate IAP values shows that a constant decrease in the IAP occurs over the length of the study for L710 leachates. Magnesium sulfate IAP values for the L310 and L610 solutions stabilize after approximately 800 days of study. Although stable magnesium sulfate IAP values are attained, the leachates arehighly undersaturated with respect to epsomite. All leachates were also highly undersaturated with respect to brucite ($Mg(OH)_2$), supporting the conclusion that soluble Mg results from brucite dissolution (Robl 1989).

Sullivan et al. (1988b) examined the equilibrium weathering of New Albany and Chattanooga Shales using the WATEQFC model. They found that oil shale extracts under moderately reducing and acidic conditions were saturated with respect to melanterite ($FeSO_4 \cdot 7H_2O$). Although SO_4^{2-} activities are directly related to those of Fe^{2+}, the L710 leachates approach saturation with respect to melanterite from supersaturation (Figure 5). Leachates from the lysimeters containing retorted oil shales (L310 and L610) are, in general, undersaturated with respect to the ferrous sulfate and the calculated IAP values are highly variable with time.

As previously noted, predicted Fe^{3+} activities are directly related and highly sensitive to the redox status of the leachates. Because leachate redox values for model input were estimated and not measured values, conclusions based on GEOCHEM predicted Fe^{3+} activities must be interpreted cautiously. The ferric iron sulfate equilibria illustrates that SO_4^{2-} and Fe^{3+} activities are directly related. Lysimeter leachate equilibria with respect to some ferric sulfate minerals commonly associated with acid sulfate weathering are also illustrated in Figure 6. In general, the calculated IAP values for Na- and K-jarosite are highly scattered and suggest that the lysimeter leachates are undersaturated with respect to these minerals.

The lysimeter leachates were also evaluated with respect to a basic iron sulfate solid phase (Fe-jurbanite, $FeSO_4OH$), whose stoichiometry and stability were suggested by Sullivan et al. (1988a) from eastern oil shale equilibrium leachates. Lysimeter L710 leachates were supersaturated with respect to Fe-jurbanite and calculated IAP values approached a constant value after approximately 800 days of study. Given the assumptions used to predict Fe^{3+} activities, it is plausable to conclude that the L710 leachates approach saturation with respect to Fe-jurbanite. Further, differences in the L710 IAP values and the Fe-jurbanite K_{sp} may also result from errors associated with the noncritical determination of K_{sp}. Lysimeter L310 and L610 leachates were also supersaturated with respect to Fe-jurbanite. However, the IAP values for these leachates were variable with time. Finally, The Fe^{3+} equilibria data suggest that the lysimeter leachates

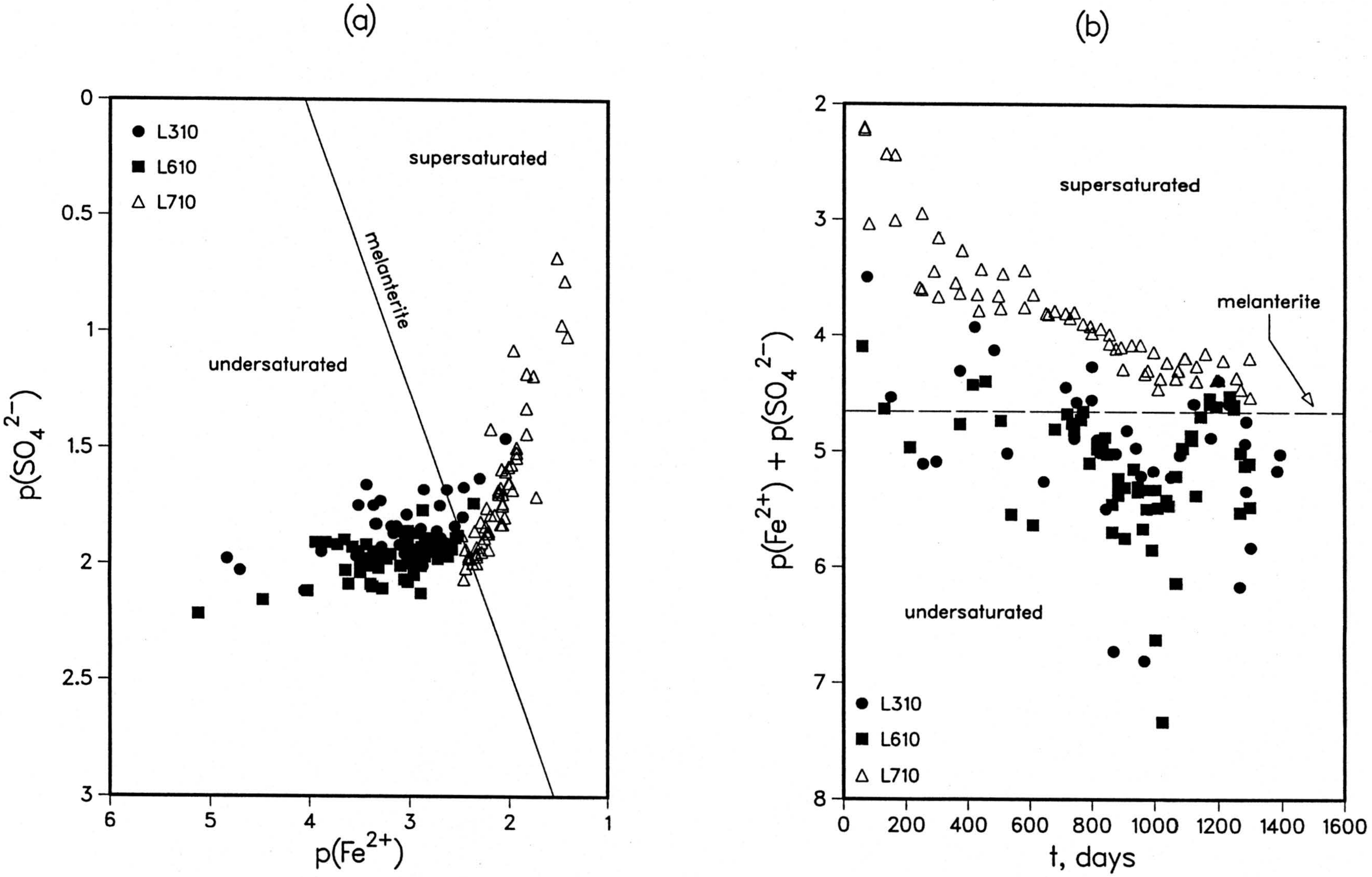

Figure 5. Ferrous Sulfate Equilibria in Lysimeter Leachates

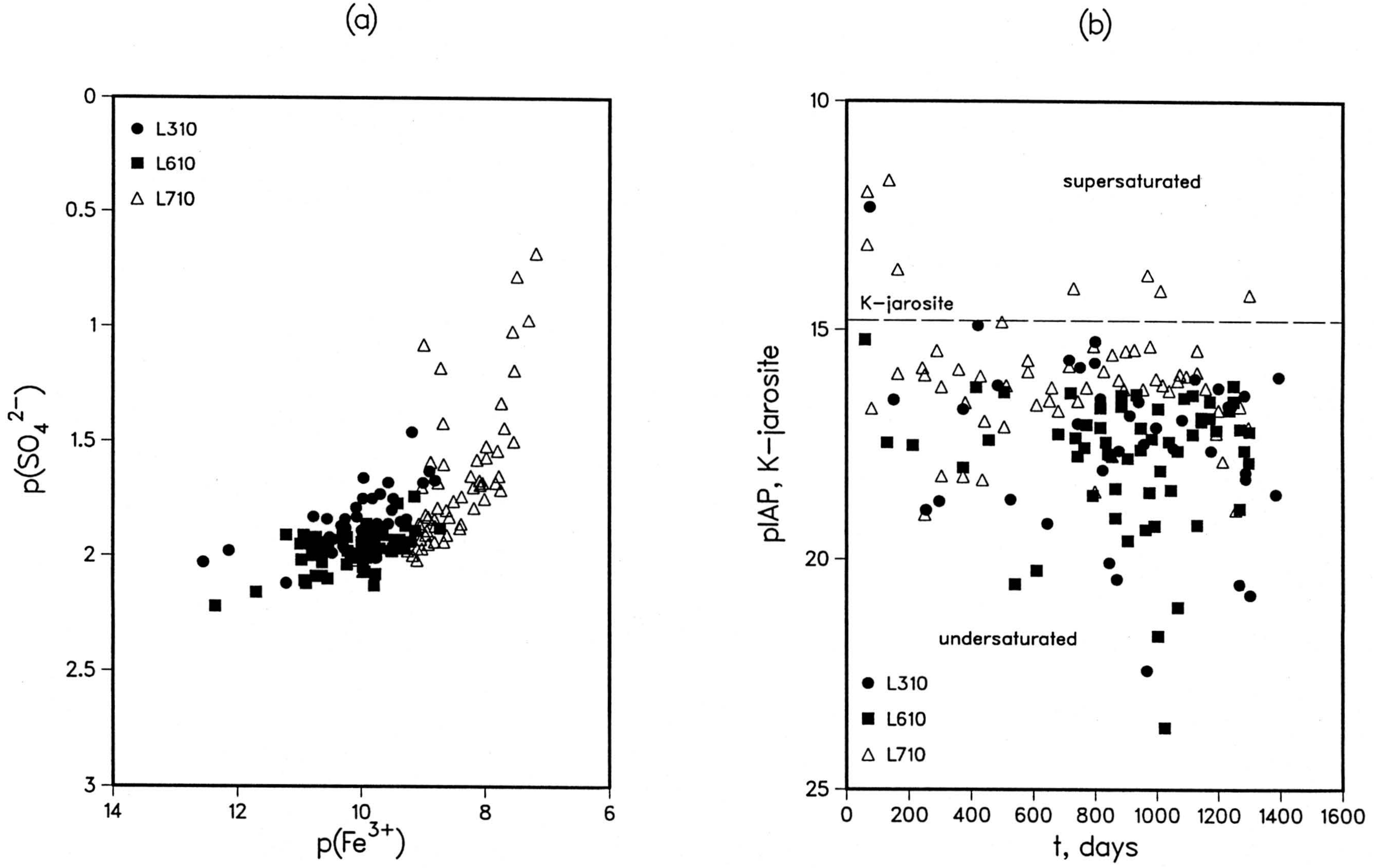

Figure 6. Ferric Sulfate Equilibria in Lysimeter Leachates

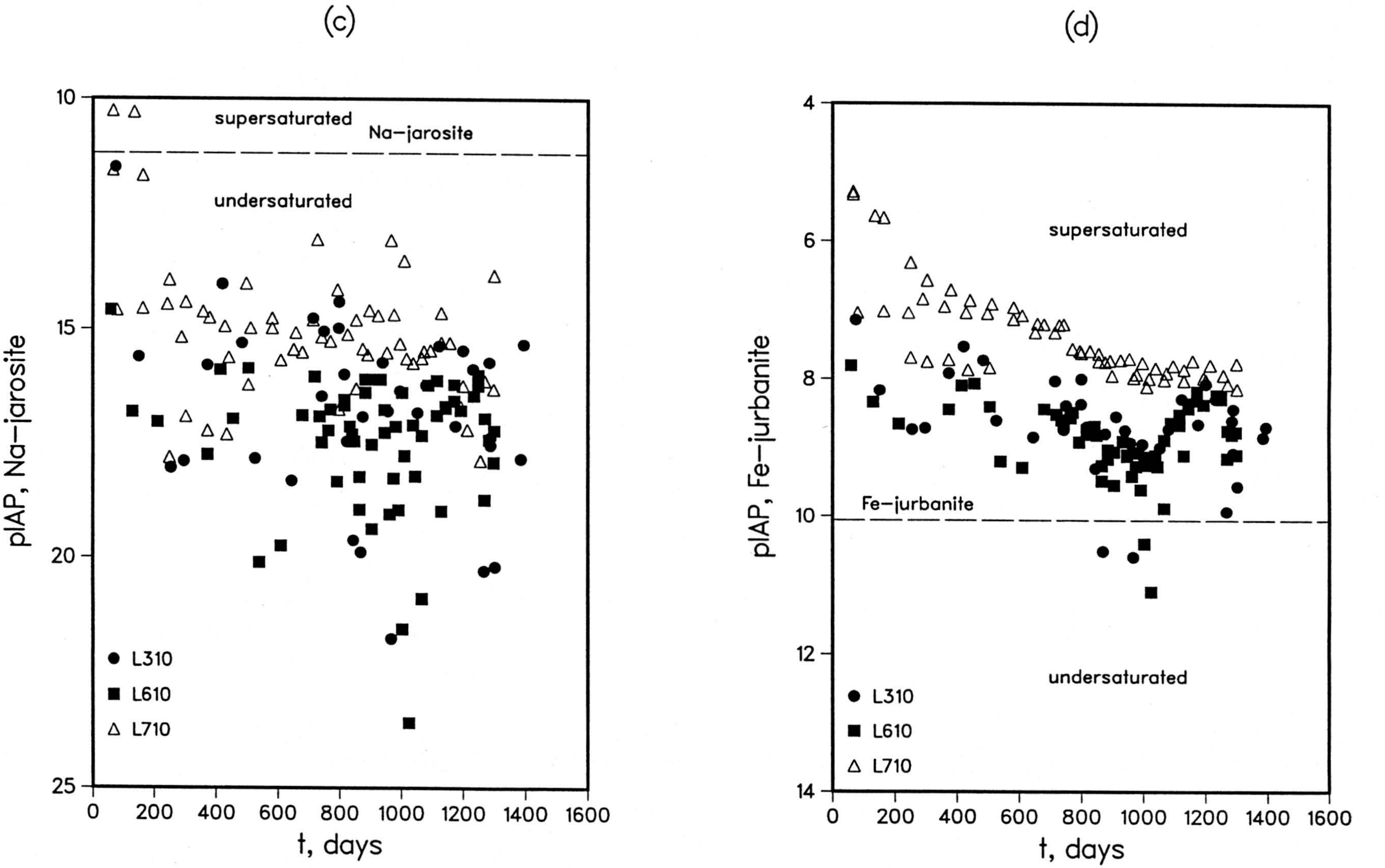

Figure 6 continued. Ferric Sulfate Equilibria in Lysimeter Leachates.

may be saturated with respect to goethite (Figure 7), again supporting the observations of Robl (1989).

Metal sulfate equilibria relationships for Mn, Cu, Cd, Zn, and Ni (Figures 8 through 12, respectively) were similar. In general, metal ion and SO_4^{2-} activities in L710 leachates are directly related. Metal ion and SO_4^{2-} activities in L310 and L610 leachates are directly related or unrelated (e.g., Cu^{2+}). Metal sulfate IAP values for L710 leachates continuously decrease with time. Metal sulfate IAP values for the L310 and L610 leachates also decrease with time, although notto the same extent as L710 leachates, and the calculated IAP values appear to stabilize after approximately 800 days of study. Irrespective of the predicted variances in calculated IAP values, all leachates are highly undersaturated with respect to even the most stable metal sulfates (Table 2).

Reddy et al. (1988a) examined the solubility relationships of zinc associated with New Albany and Chattanooga Shale leachates. Zinc activities in leachates with pH values greater than 7.0 were supported by Zn_2SiO_4 (willemite), whereas zinc activities in leachates with pH values less than 5.0 were supported by $ZnFe_2O_4$ (franklinite). The status of the lysimeter leachates with respect to franklinite and $NiFe_2O_4$ (trevorite) is illustrated in Figure 13. The diagrams show that the leachates are undersaturated with respect to the ferrite phases. The leachates were also undersaturated with respect to the Cu-ferrite solid phase (not shown). Because there are potential errors associated with the predicted Fe^{3+} activity values lysimeter leachate saturation with respect to the metal ferrites, especially franklinite, cannot be ruled out.

Aluminum chemistry was evaluated with respect to a number of solids predicted to occur in weathering acid sulfate materials (Nordstrom 1982; Sullivan et al. 1988a, b). The status of the lysimeter leachates with respect to aluminosilicates could not be determined because soluble silica concentrations were not determined (Robl 1989). The pH versus $p(Al^{3+})$ activity diagram (Figure 14) suggests that Al^{3+} in L710 leachates may be controlled by alunite $[KAl_3(SO_4)_2(OH)_6]$ or jurbanite ($AlSO_4OH$). Lysimeter L310 and L610 leachates are undersaturated with respect to basaluminite ($Al_4SO_4(OH)_{10}$) and supersaturated with respect to alunite. All leachates are undersaturated with respect to gibbsite.

Plots of mineral IAP values versus study duration show that soluble Al in the lysimeter leachates is not supported by the basic aluminum sulfates. In general, L310 and L610 leachates are supersaturated with respect to alunite and jurbanite and undersaturated with respect to basaluminite. Leachate from L710 are undersaturated with respect to alunite and basaluminite and become undersaturated with respect to jurbanite with study duration. This latter condition is inconsistent with the findings of Sullivan et al. (1988a, b). They report that acidic New Albany and Chattanooga Shale leachates are saturated with respect to jurbanite.

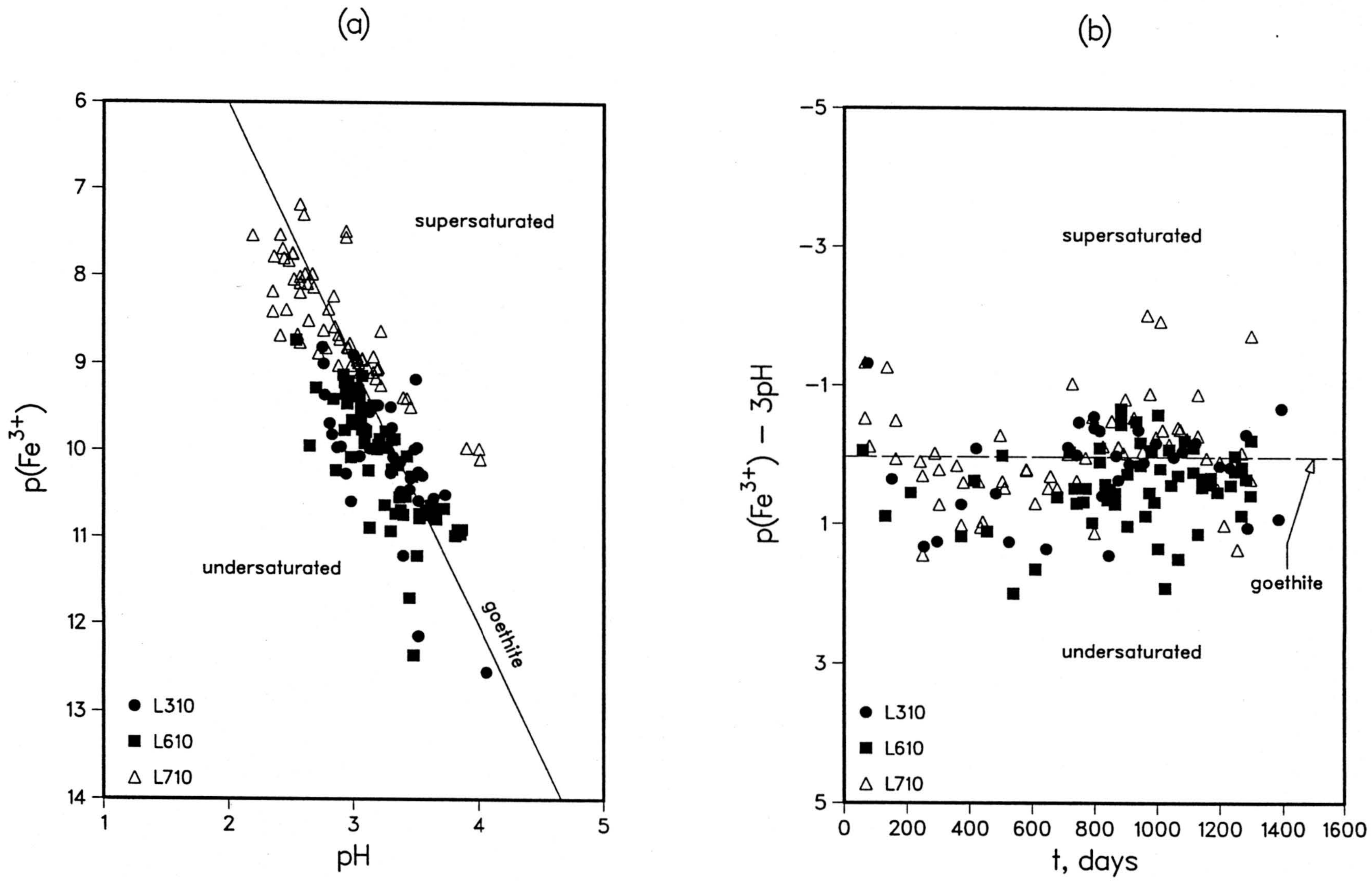

Figure 7. Ferric Hydroxide Equilibria in Lysimeter Leachates

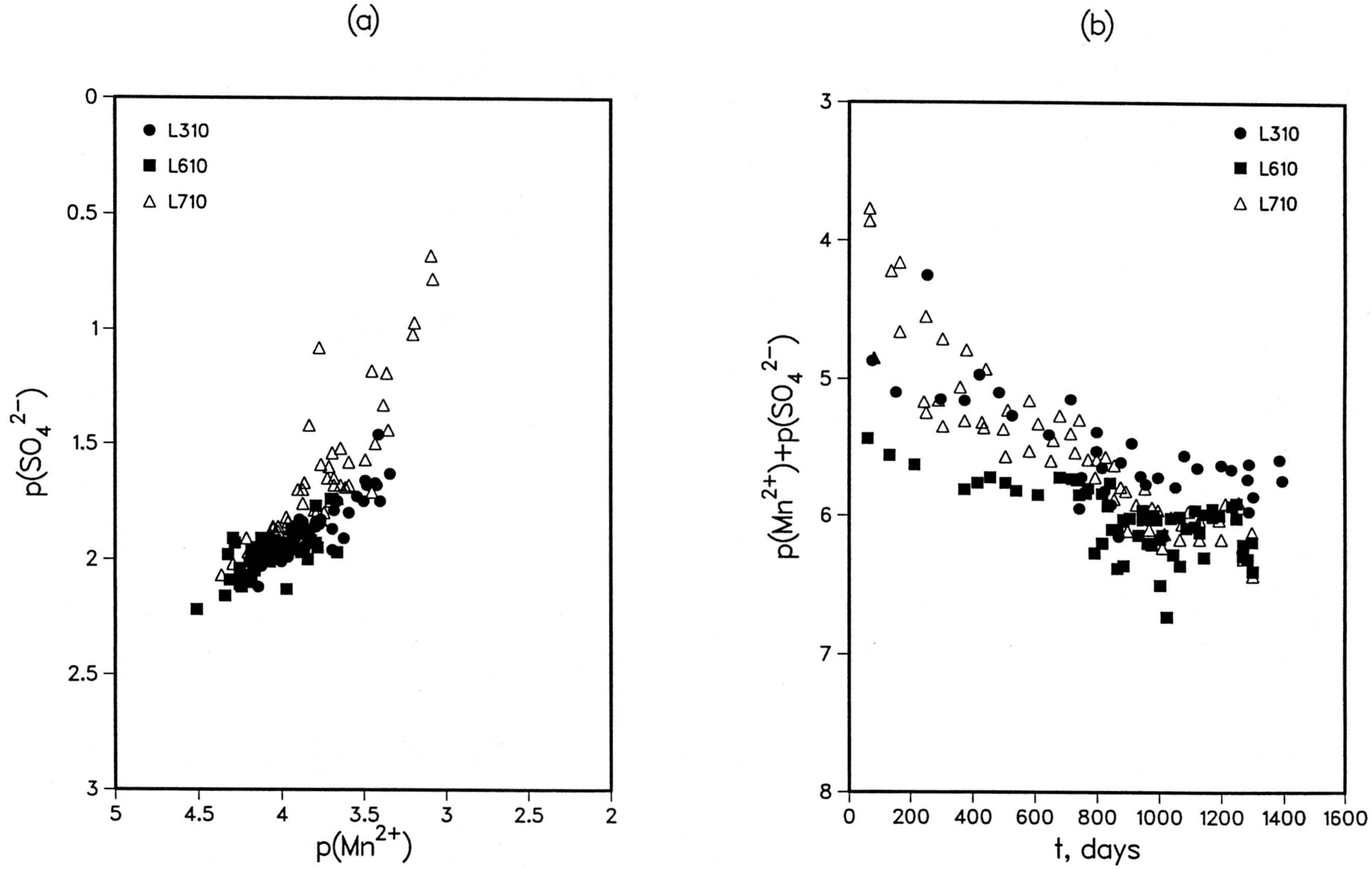

Figure 8. Manganese Sulfate Equilibria in Lysimeter Leachates

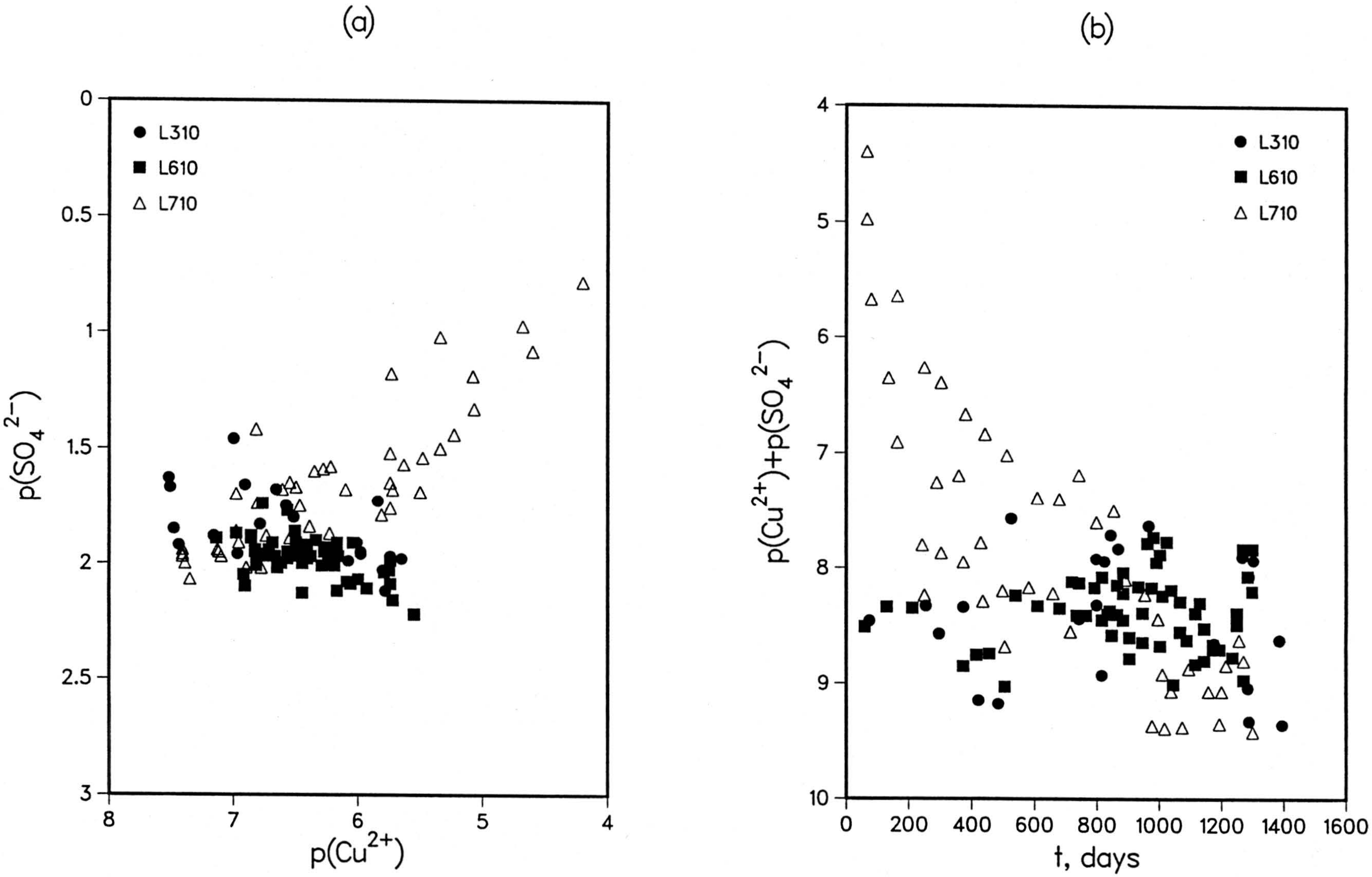

Figure 9. Copper Sulfate Equilibria in Lysimeter Leachates

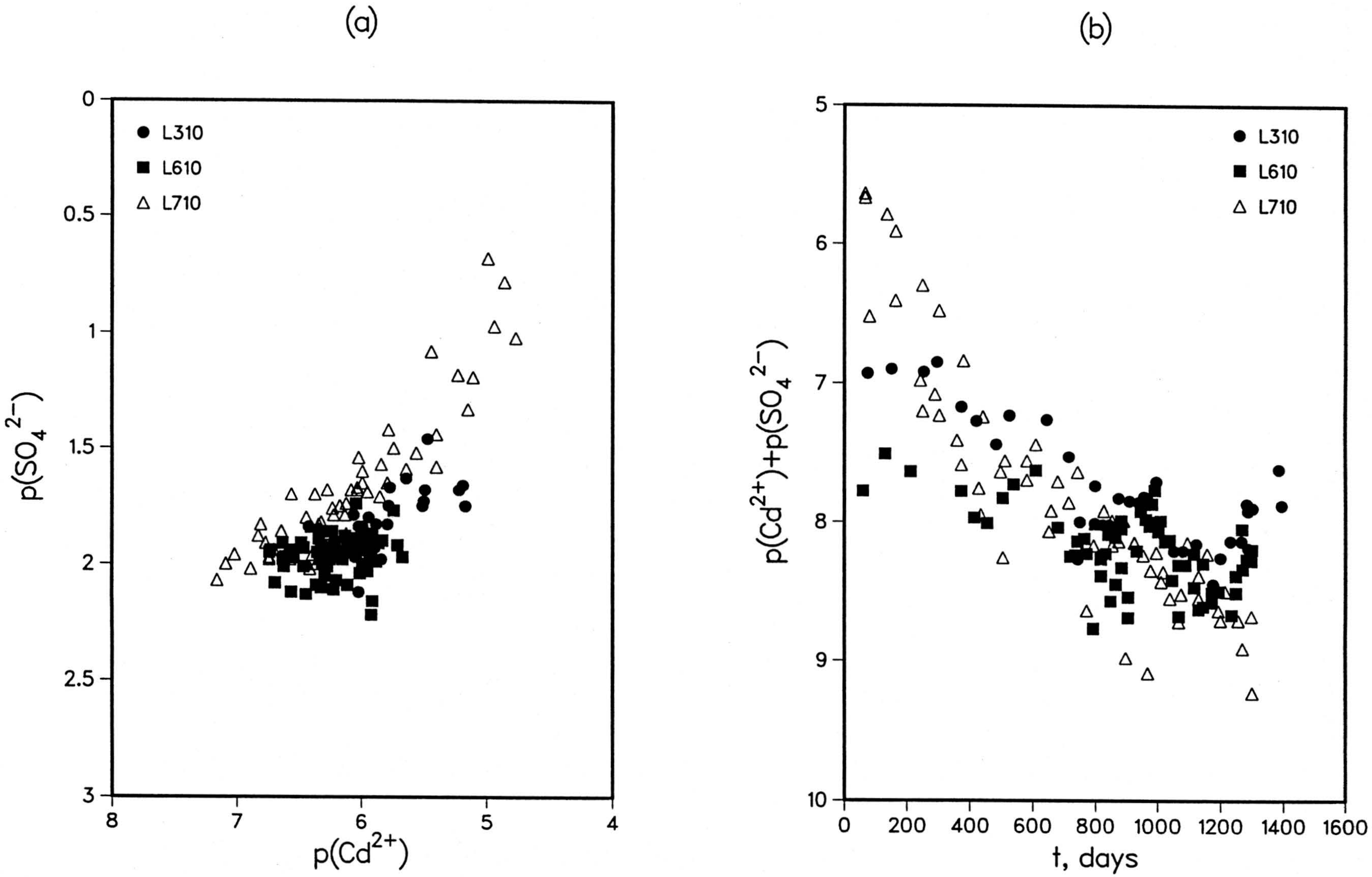

Figure 10. Cadmium Sulfate Equilibria in Lysimeter Leachates

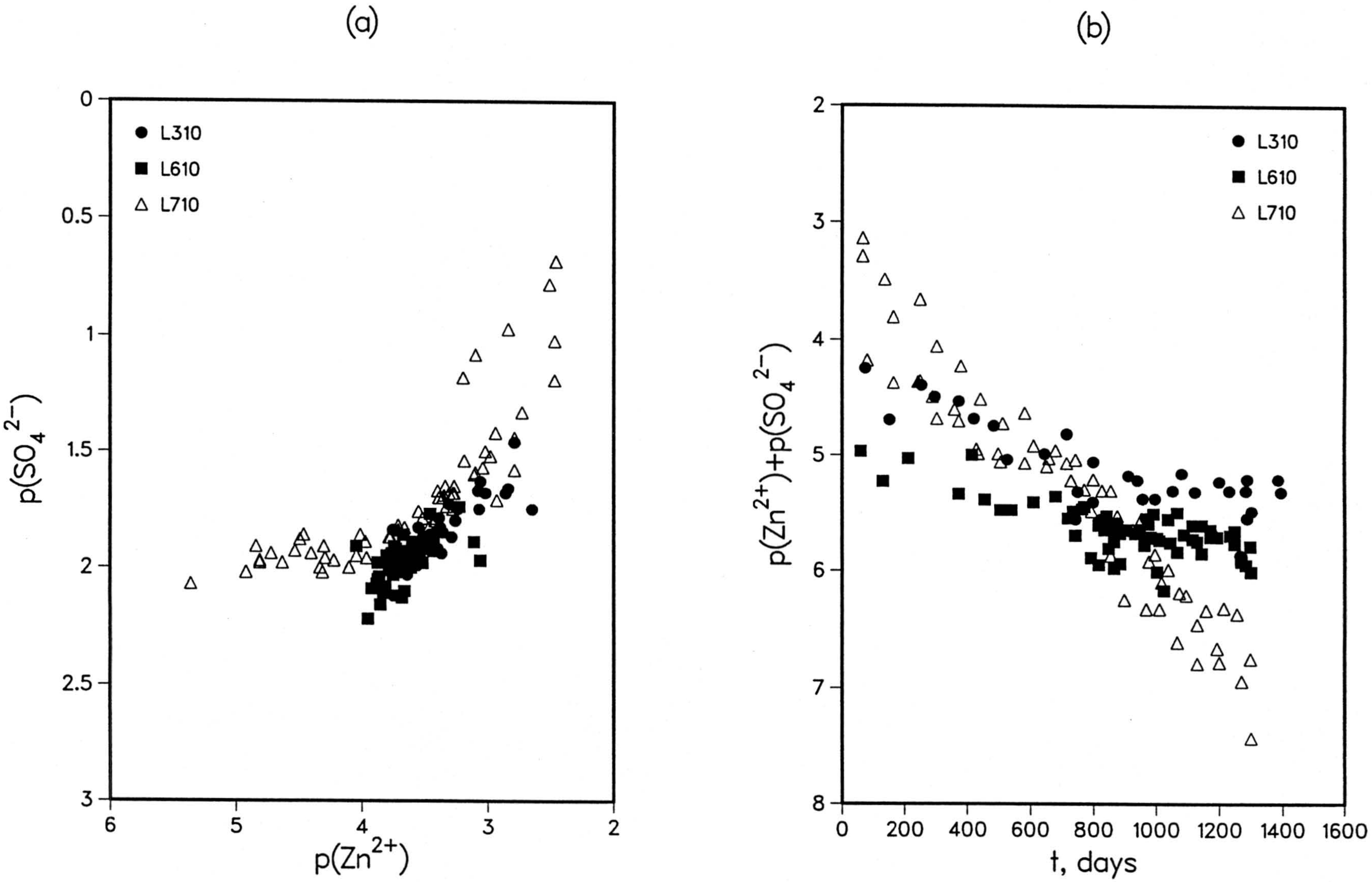

Figure 11. Zinc Sulfate Equilibria in Lysimeter Leachates

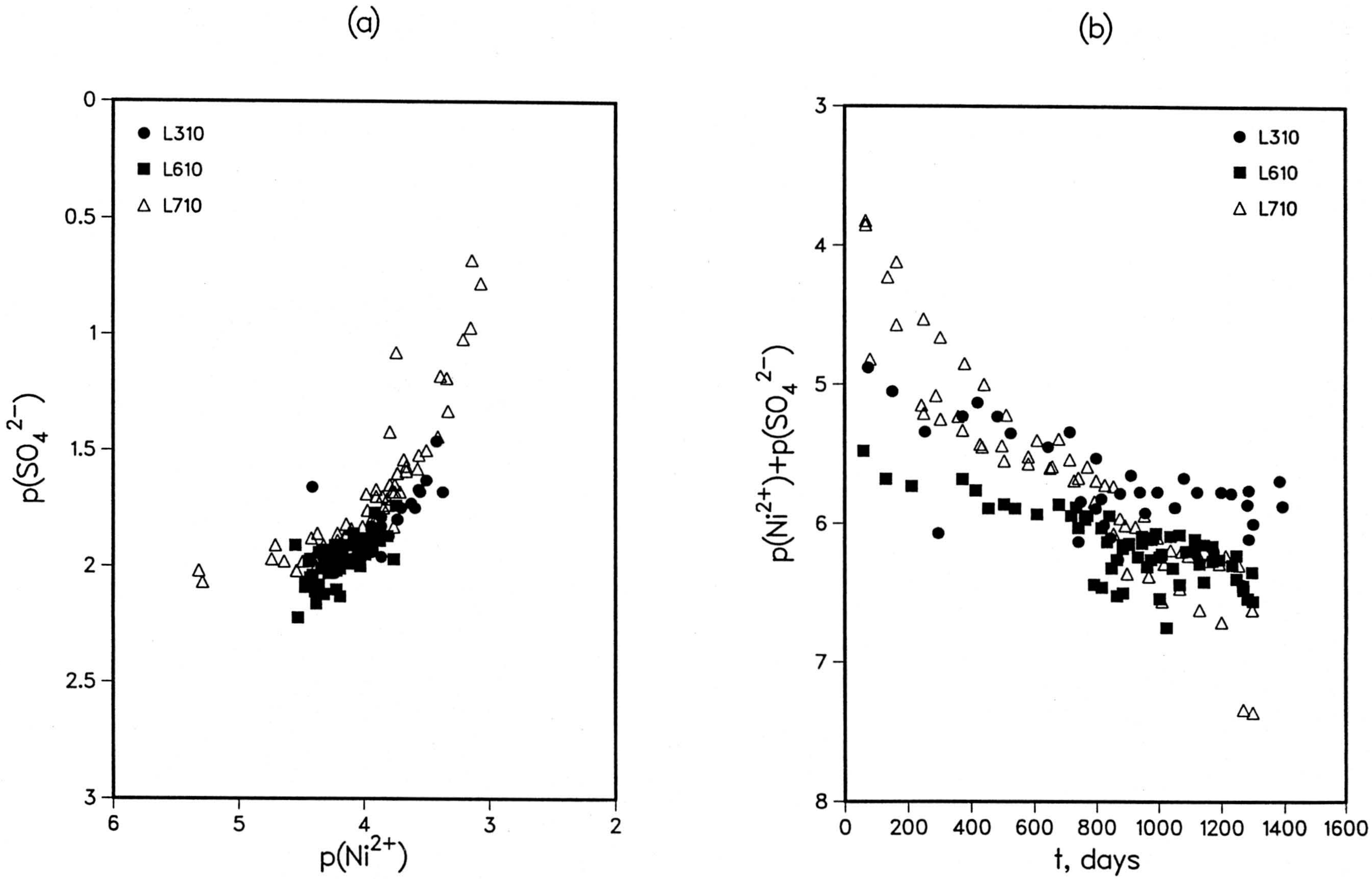

Figure 12. Nickel Sulfate Equilibria in Lysimeter Leachates

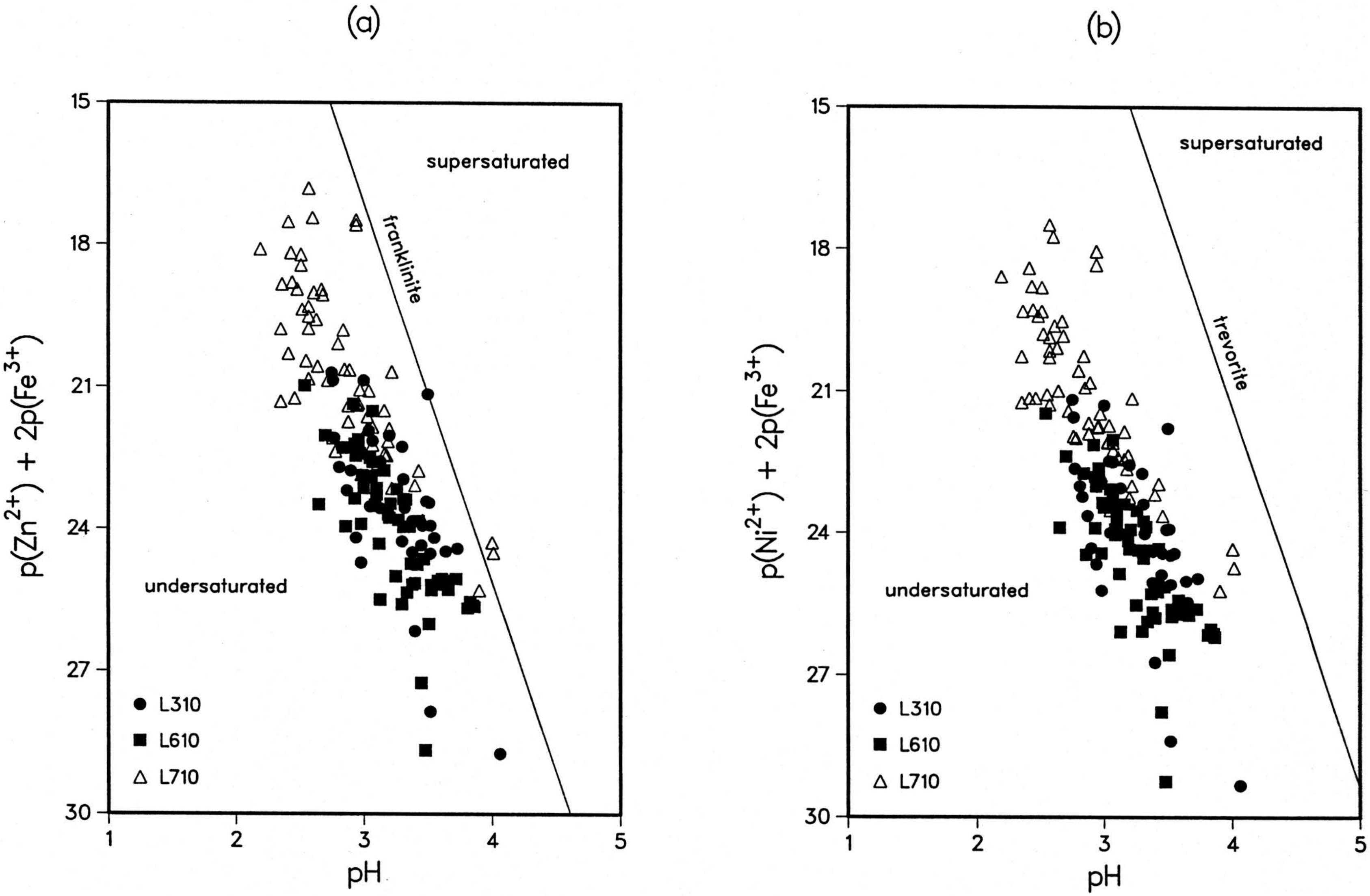

Figure 13. Zinc and Nickel Ferrite Equilibria in Lysimeter Leachates

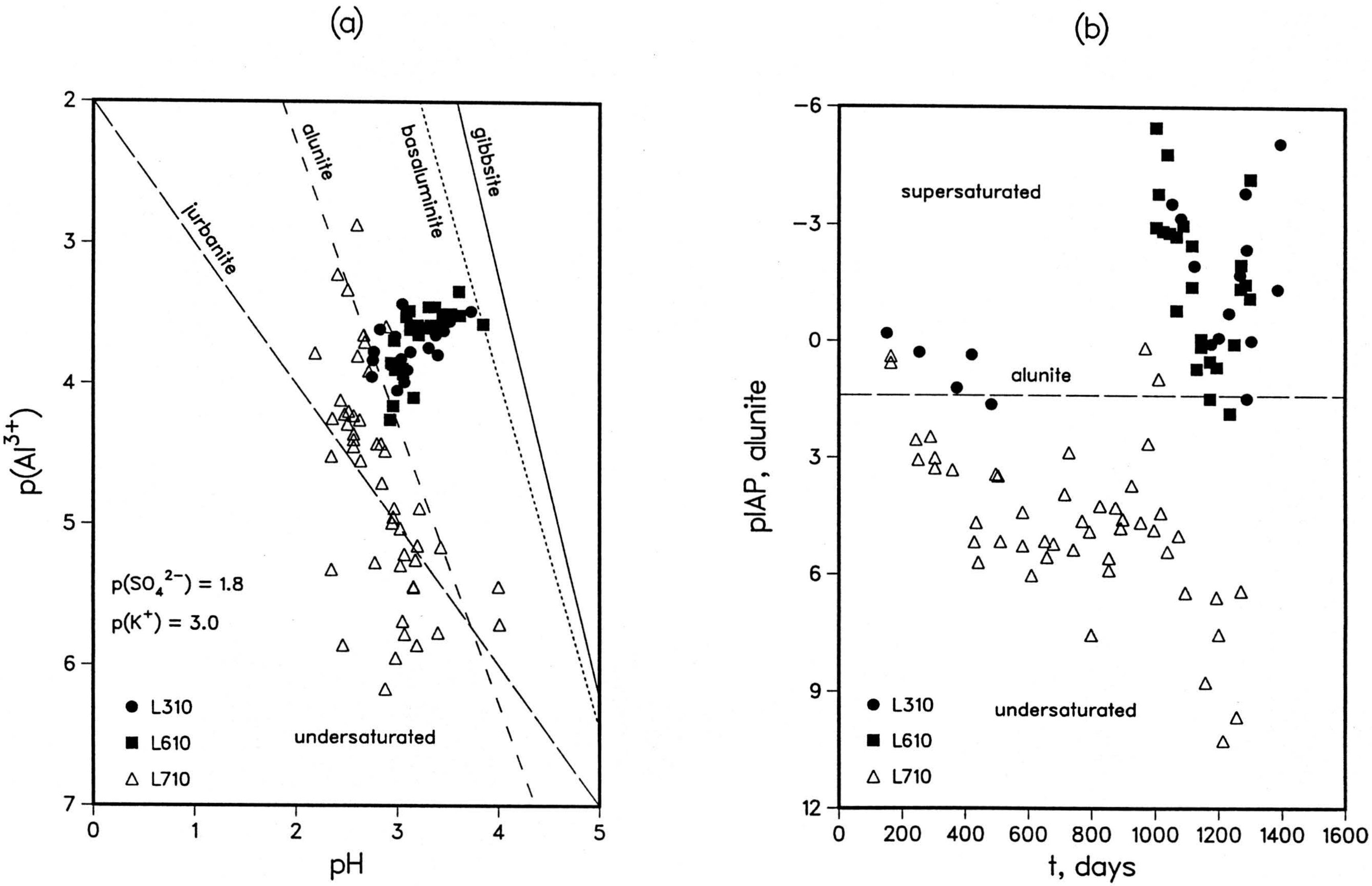

Figure 14. Aluminum Sulfate Equilibria in Lysimeter Leachates

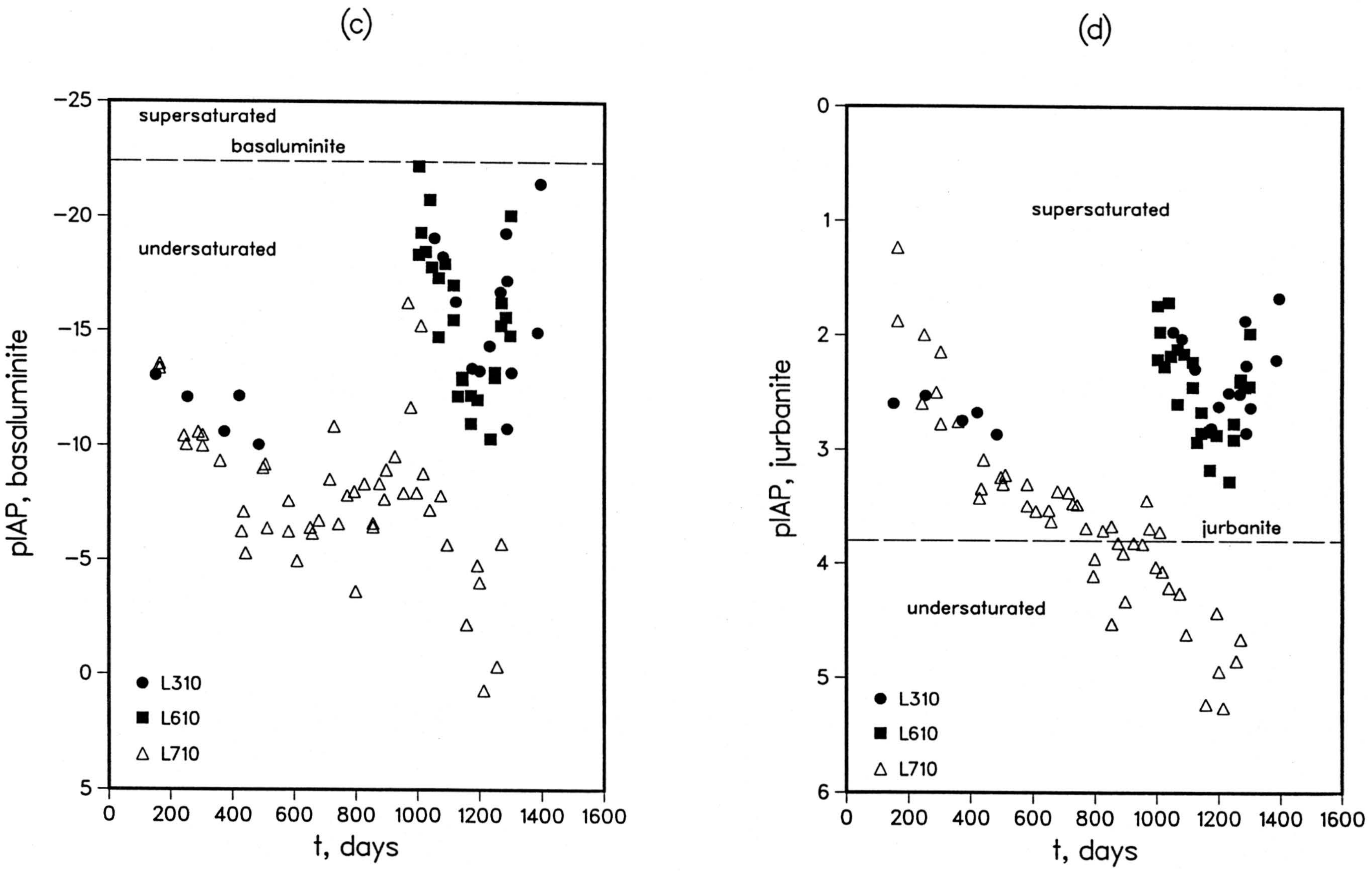

Figure 14 continued. Aluminum Sulfate Equilibria in Lysimeter Leachates

Molybdate activities in the lysimeter leachates are supported by molybdite (MoO_3) and molybdic acid (H_2MoO_4(c)) (Figure 15). The status of the leachates with respect to powellite ($CaMoO_4$) and lead molybdate was also examined. All leachates were undersaturated with respect to powellite and supersaturated with respect to lead molybdate (data not shown).

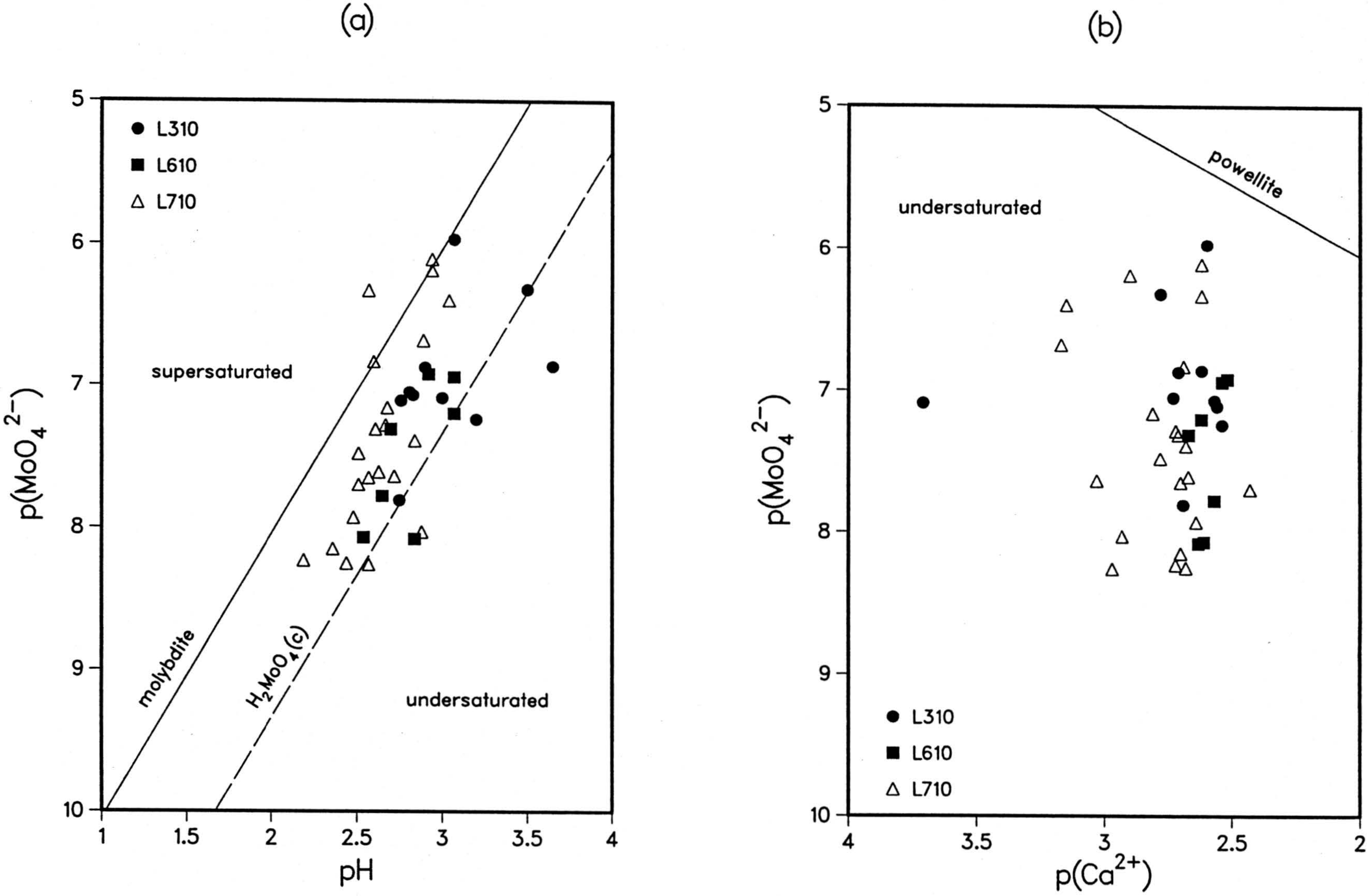

Figure 15. Molybdate Equilibria in Lysimeter Leachates

CONCLUSIONS

Results of the chemical equilibria model analysis of leachates from field lysimeters provided a more detailed characterization of the chemistry of oil shale materials. The aqueous chemistry of an eastern oil shale, retorted eastern oil shale, and an oil shale fines/retorted oil shale mixture is dominated by free ionic metal species and metal sulfate ion pairs. Activity diagrams show that free-metal ion activities (with the exception of Ca^{2+}) are directly related to SO_4^{2-} activities. This suggests that the aqueous activities of the metals examined are not supported by metal sulfate solid phases. However, an examination of metal sulfate ion activity products as a function of time show that the IAPs approach constant values after approximately 800 days of the field study. For the great majority of the metals examined, the IAP values suggest leachate undersaturation with respect to even the most stable metal sulfate phases. Leachates from all three materials are predicted by GEOCHEM to approach equilibrium with respect to gypsum and goethite. In addition, leachates from the oil shale lysimeter are predicted by GEOCHEM to approach equilibrium with respect to melanterite, Fe-jurbanite, franklinite, molybdite, and molybdic acid. Aluminum activities in all three lysimeter leachates fall within the stability region of several basic aluminum sulfates. However, Al^{3+} activities in the lysimeter leachates are not supported by sulfate phases.

ACKNOWLEDGMENTS

I wish to thank Dr. Thomas Robl for providing the leachate concentration data for model analysis and the United States Department of Energy for funding this work under Cooperative Agreement Number DE-FC21-86MC11076.

DISCLAIMER

REFERENCES

Adams, F., and Z. Rawajfih, 1977, Basaluminite and Alunite: A Possible Cause of Sulfate Retention by Acid Soils. *Soil Sci. Soc. Am. J.*, 41: 686-692.

Ball, J.W., D.K. Nordstrom, and E.A. Jenne, 1980, Additional and Revised Thermodynamical Data and Computer Code for WATEQ2 - A Computerized Chemical Model for Trace and Major Element Speciation and Mineral Equilibria of Natural Waters. U.S. Geological Survey, Water Resources Investigation 78-116.

Esmaili, E., R.B. Carroll, and L.P. Jackson, 1985, Assessing Potential Trace Metal Leachability of Retorted Oil Shale by Complexometric Agents. 18th Oil Shale Symposium Proceedings, Golden, CO, 326-337.

Essington, M.E., 1987, Modeling Fluoride Chemistry in Hydrated and Recarbonated Spent Western Oil Shales. 1987 Eastern Oil Shale Symposium Proceedings, Lexington, KY, 21-33.

Essington, M.E., Calcium Molybdate Solubility in Spent Oil Shale and a Preliminary Evaluation of the Association Constants for the Formation of $CaMoO_4^0$(aq), $KMoO_4^-$(aq), and $NaMoO_4^-$(aq). *Environ. Sci. Technol.*, in press.

Essington, M.E., and L.K. Spackman, 1986, Recarbonation of Retorted Oil Shale: The Influence on Mineralogy and Leachate Chemistry. Laramie, WY, DOE Report DOE/FE/60177-2433.

Essington, M.E., and L.K. Spackman, 1988, Inorganic Geochemical Investigations of Spent Oil Shales. Laramie, WY, DOE Report DOE/MC/11076-2701.

Essington, M.E., L.K. Spackman, J.D. Harbour, and K.D. Hartman, 1987, Physical and Chemical Characteristics of Retorted and Combusted Western Reference Oil Shale. Laramie, WY, DOE Report DOE/MC/11076-2453.

Felmy, A.R., D.Girvin, and E.A. Jenne, 1984, MINTEQ: A Computer Program for Calculating Aqueous Geochemical Equilibria. Athens, GA, Environmental Protection Agency.

Koppenaal, D.W., R.R Kruspe, T.L. Robl, K. Cisler, and D.L. Allen, 1984, The Examination of Eastern Oil Shale Disposal Problems - The Hope Creek Field Study. 1984 Eastern Oil Shale Symposium Proceedings, Lexington, KY, 199-206.

Lindsay, W.L., 1979, *Chemical Equilibria in Soils*. John Wiley and Sons, New York, NY, 449 p.

Mattigod, S.V., and G. Sposito, 1979, Chemical Modeling of Trace Metal Equilibria in Contaminated Soil Solutions Using the Computer Program GEOCHEM, in Jenne, E.A., ed., Chemical Modeling in Aqueous Systems, ACS Symposium Series No. 93, American Chemical Society, Washington, DC, 837-856.

Naumov, G.B., B.N. Ryzhenko, and I.L. Khodakovsky, 1974, Handbook of Thermodynamic Data. U. S. Geological Survey, PB226722.

Nordstrom, D.K., 1982, The Effect of Sulfate on Aluminum Concentrations in Natural Waters: Some Stability Relations in the System Al_2O_3-SO_3-H_2O at 298 K. Geochim. Cosmochim. Acta, 46: 681-692.

Parkhurst, D.L., D.C. Thorstenson, and L.N. Plummer, 1980, PHREEQE - A Computer Program for Geochemical Calculations. U.S. Geological Survey, Water Resources Investigation 80-96.

Reddy, K.J., and J.I. Drever, 1987, Geochemical Modeling Research Related to the Surface Disposal of Processed Oil Shale Solid Waste. Laramie, WY, DOE Report DOE/MC/11076-2443.

Reddy, K.J., and W.L. Lindsay, 1986, The Solubility Relationships of Calciuum and Magnesium Minerals in Processed Oil Shale. J. Environ. Qual., 15: 1-4.

Reddy, K.J., W.L. Lindsay, F.W. Boyle, and E.F. Redente, 1986, Solubility Relationships and Mineral Transformations Associated with Recarbonation of Retorted Shales. J. Environ. Qual., 15: 129-133.

Reddy, K.J., P.J. Sullivan, and J.L. Yelton, 1988a, Solubility Relationships of Zinc Associated with Acid Mine Drainage. J. Environ. Qual., 17: 712-714.

Reddy, K.J., J.I. Drever, and V.R. Hasfurther, 1988b, Application of Geochemical Models to Oil Shale Solid Waste. Laramie, WY, DOE report in press.

Robl, T.L., 1989, Field and Laboratory Leaching Studies of Retorted Kentucky Oil Shale. Lexington, KY, DOE report in press.

Robl, T.L., G. Thomas, K. Cisler, and D. Koppenaal, 1985, Leaching Characteristics of Eastern Oil Shale: First Year Data Summary of the Hope Creek Study. 1985 Eastern Oil Shale Symposium Proceedings, Lexington, KY, 117-129.

Robl, T.L., J. Obley, G. Thomas, W. Jones, and M. Shirav, 1986, Elemental Release Characteristics of Eastern Oil Shales: Comparison of Field and Laboratory Results. 1986 Eastern Oil Shale Symposium Proceedings, Lexington, KY, 231-243.

Robl, T., J. Obley, B. Schram, G. Thomas, and J. Kung, 1987, Leachate Composition and Elemental Release Pattern for Easternm Oil Shale Materials from the Hope Creek Field Study. 1987 Eastern OIl Shale Symposium Proceedings, Lexington, KY, 59-66.

Robl, T.L., L.S. Barron, W. Schram, and G. Thomas, 1988, Final Summary of Data from the Hope Creek Field Lysimeter Study. 1988 Eastern Oil Shale Symposium Proceedings, Lexington, KY, 115-121.

Runnells, D.D., and R.D. Lundberg, 1981, Hydrogeochemical exploration for Uranium Deposits: Use of the Computer Model WATEQFC. J. Geochem. Explor., 15: 37-50.

Saether, O.M., and D.D. Runnells, 1980, Geochemistry of Fluorine in Oil Shale Leachates. 13th Oil Shale Symposium Proceedings, Golden, CO, 362-368.

Spackman, L.K., K.D. Hartman, J.D. Harbour, and M.E. Essington, Adsorption of Oxyanions by Spent Western Oil Shale: I. Arsenate. Environ. Geol. Water Sci., in press.

Spackman, L.K., K.D. Hartman, J.D. Harbour, and M.E. Essington, Adsorption of Oxyanions by Spent Western Oil Shale: II. Selenite. Environ. Geol. Water Sci., in press.

Sposito, G., and S.V. Mattigod, 1980, GEOCHEM: A Computer Program for the Calculation of Chemical Equilibria in Soil Solutions and Other Natural Water Systems. University of California, Riverside, CA.

Stollenwerk, K.G., and D.D. Runnells, 1981, Composition of Leachate from Surface-Retorted and Unretorted Colorado Oil Shale. Environ. Sci. Technol., 15: 1340-46.

Sullivan, P.J., J.L. Yelton, and K.J. Reddy, 1988a, Solubility Relationships of Aluminum and Iron Minerals Associated with Acid Mine Drainage. Environ. Geol. Water Sci., 11: 283-287.

Sullivan, P.J., J.L. Yelton, and K.J. Reddy, 1988b, Iron Sulfide Oxidation and the Chemistry of Acid Generation. Environ. Geol. Water Sci., 11: 289-295.

Truesdell, A.H., and B.F. Jones, 1974, WATEQ - A Computer Program for Calculating Chemical Equilibria in Natural Water. J. Res. U. S. Geol. Surv., 2:233-248.

APPENDIX A

Chemical Data Used in the Geochemical Model Evaluations

Table A1. Lysimeter L310 Data Used in the GEOCHEM Evaluations (-log mol L^{-1}, unless noted otherwise)

Sample Number:	9L	20L	31L	42L	53L	64L	75L	86L
Elapsed Time, days:	74	151	254	296	373	421	484	526
pH (units)	3.50	3.07	2.83	2.90	2.76	3.00	2.75	2.81
pe (units)	5.50	5.93	6.17	6.10	6.24	6.00	6.25	6.19
Ca	2.025	1.925	1.923	2.032	1.889	3.027	2.019	2.102
Mg	1.262	1.321	1.416	1.360	1.377	1.394	1.398	1.670
K	2.673	2.735	2.793	2.779	2.753	2.780	2.772	2.873
Na	1.839	1.816	1.884	1.917	1.824	1.877	1.865	2.009
ΣFe	1.314	2.205	2.726	2.783	1.980	1.640	1.809	2.683
Mn	2.650	2.740	2.842	2.816	2.810	2.654	2.758	2.907
Cu	6.201	9.000	5.900	6.201	5.958	6.803	6.803	5.180
Cd	4.517	4.434	4.423	4.400	4.710	4.841	4.986	4.774
Zn	1.991	2.310	1.964	2.127	2.161	2.340	2.381	2.648
Ni	2.658	2.689	2.936	3.735	2.882	2.814	2.888	2.990
Pb	5.271	4.785	5.538	4.974	4.918	5.471	9.000	4.901
Al	9.000	2.431	2.109	9.000	2.288	2.477	2.402	9.000
SO_4	0.768	1.025	1.088	1.029	1.020	0.985	1.014	1.155
$B(OH)_4$	3.160	3.425	3.545	3.474	3.293	3.278	3.249	3.318
MoO_4	4.892	4.224	5.028	4.941	4.982	5.329	5.681	5.028

Table A1. Lysimeter L310 Data Used in the GEOCHEM Evaluations (-log mol L^{-1}, unless noted otherwise) (continued)

Sample Number:	108L	119L	130L	141L	152L	163L	174L	185L
Elapsed Time, days:	645	715	750	816	876	940	996	1052
pH (units)	2.87	3.20	3.49	3.55	3.30	3.64	3.65	3.52
pe (units)	6.13	5.80	5.51	5.45	5.70	5.36	5.35	5.48
Ca	2.035	1.902	1.959	1.980	1.980	2.071	1.950	1.969
Mg	1.580	1.365	1.795	2.005	1.732	1.714	1.773	1.817
K	2.882	2.749	2.852	2.868	2.818	2.909	2.893	2.920
Na	1.964	1.855	2.083	2.366	2.106	2.083	2.131	2.185
ΣFe	2.908	2.085	2.066	2.367	2.543	2.492	2.702	2.679
Mn	3.032	2.762	3.172	3.077	3.096	3.196	3.221	3.221
Cu	9.000	9.000	9.000	6.326	9.000	9.000	9.000	9.000
Cd	4.796	5.051	5.352	5.574	5.206	5.238	5.092	5.546
Zn	2.585	2.404	2.736	2.970	3.037	2.669	2.838	2.702
Ni	3.070	2.949	3.292	3.250	3.263	3.263	3.263	3.306
Pb	9.000	5.839	9.000	9.000	9.000	9.000	9.000	9.000
Al	9.000	9.000	9.000	9.000	9.000	9.000	9.000	2.130
SO_4	1.167	1.117	1.294	1.409	1.254	1.260	1.254	1.319
$B(OH)_4$	3.454	3.432	3.443	3.490	3.381	3.443	3.449	3.502
MoO_4	9.000	5.681	9.000	9.000	9.000	9.000	5.505	9.000

Table A1. Lysimeter L310 Data Used in the GEOCHEM Evaluations (-log mol L^{-1}, unless noted otherwise) (continued)

Sample Number:	190L	196L	207L	218L	2C	4C	6C	8C
Elapsed Time, days:	1080	1122	1199	1283	799	911	957	1231
pH (units)	3.46	3.31	3.04	3.52	3.30	3.32	3.45	3.13
pe (units)	5.54	5.69	5.96	5.48	5.70	5.68	5.55	5.87
Ca	1.990	1.969	1.959	2.012	2.012	1.922	1.969	1.969
Mg	1.687	1.732	1.723	1.842	1.553	1.608	1.829	1.678
K	2.855	2.831	2.864	2.876	2.796	2.802	2.829	2.871
Na	2.131	2.131	2.061	2.185	1.930	2.039	2.157	2.106
ΣFe	2.543	2.114	1.921	2.446	1.813	2.385	2.706	2.114
Mn	3.041	3.138	3.138	3.221	2.901	3.000	3.235	3.160
Cu	9.000	9.000	9.000	6.502	5.803	9.000	9.000	9.000
Cd	5.604	5.559	5.671	5.280	5.148	5.273	5.206	5.546
Zn	2.611	2.774	2.702	2.766	2.537	2.669	2.815	2.774
Ni	3.156	3.263	3.277	3.354	3.044	3.178	3.388	3.277
Pb	9.000	9.000	9.000	9.000	9.000	9.000	9.000	9.000
Al	2.176	2.285	2.352	2.089	9.000	9.000	9.000	2.317
SO_4	1.251	1.238	1.212	1.281	1.156	1.179	1.375	1.236
$B(OH)_4$	3.466	3.390	3.335	3.421	3.318	3.278	3.381	3.411
MoO_4	9.000	9.000	9.000	9.000	9.000	9.000	9.000	9.000

Table A1. Lysimeter L310 Data Used in the GEOCHEM Evaluations (-log mol L^{-1}, unless noted otherwise) (continued)

Sample Number:	10C	12C	14C	2R	4R	6R	8R	10R
Elapsed Time, days:	1287	1385	1394	743	798	824	845	869
pH (units)	2.77	3.05	3.73	3.38	3.51	3.13	2.94	4.06
pe (units)	6.23	5.95	5.27	5.62	5.49	5.87	6.06	4.94
Ca	1.969	2.012	2.078	2.012	2.012	1.980	1.980	1.990
Mg	1.696	1.714	1.674	1.939	1.842	1.894	1.953	2.107
K	2.934	2.865	2.891	2.814	2.900	2.835	2.837	2.969
Na	2.061	2.106	2.185	2.248	2.157	2.248	2.375	2.407
ΣFe	2.270	2.710	2.517	2.316	2.039	2.468	2.962	4.167
Mn	3.127	3.106	3.208	3.351	2.976	3.249	3.342	3.555
Cu	6.803	6.104	6.803	5.803	5.326	5.326	5.104	5.201
Cd	5.604	5.046	5.273	5.574	5.352	5.352	5.352	5.352
Zn	2.682	2.695	2.759	2.918	2.815	2.946	3.009	3.045
Ni	3.263	3.212	3.337	3.526	3.337	3.432	3.526	3.665
Pb	9.000	9.000	9.000	9.000	9.000	9.000	9.000	9.000
Al	2.317	1.961	2.079	9.000	9.000	9.000	9.000	9.000
SO_4	1.228	1.197	1.306	1.433	1.323	1.399	1.429	1.535
$B(OH)_4$	3.301	3.502	3.529	3.542	3.454	3.432	3.490	3.619
MoO_4	9.000	9.000	9.000	9.000	9.000	9.000	9.000	9.000

Table A1. Lysimeter L310 Data Used in the GEOCHEM Evaluations (-log mol L^{-1}, unless noted otherwise) (continued)

Sample Number:	12R	14R	16R	18R	20R
Elapsed Time, days:	967	1175	1266	1287	1301
pH (units)	3.52	3.10	3.40	3.38	2.98
pe (units)	5.48	5.90	5.60	5.62	6.02
Ca	1.950	2.012	2.012	2.035	2.012
Mg	1.939	2.043	2.116	1.971	1.881
K	3.042	2.824	2.968	2.861	2.860
Na	2.362	2.320	2.699	2.301	2.265
ΣFe	4.270	2.316	3.548	2.788	3.300
Mn	3.441	3.418	3.613	3.397	3.309
Cu	5.025	6.025	5.223	5.461	5.341
Cd	5.159	5.772	5.428	5.265	5.265
Zn	2.940	3.045	3.192	2.946	2.907
Ni	3.531	3.610	3.791	3.538	3.446
Pb	9.000	9.000	9.000	9.000	9.000
Al	9.000	2.574	2.562	2.301	2.285
SO_4	1.451	1.453	1.595	1.425	1.369
$B(OH)_4$	3.755	3.529	3.733	3.587	3.619
MoO_4	9.000	9.000	9.000	9.000	9.000

Table A2. Lysimeter L610 Data Used in the GEOCHEM Evaluations (-log mol L^{-1}, unless noted otherwise)

Sample Number:	4L	9L	12L	16L	20L	24L	28L	32L
Elapsed Time, days:	720	792	816	848	865	885	905	933
pH (units)	3.31	2.93	3.47	3.10	3.34	3.86	3.42	3.72
pe (units)	5.69	6.07	5.53	5.90	5.66	5.14	5.58	5.28
Ca	1.969	2.071	2.141	2.001	2.047	2.047	1.980	2.035
Mg	1.923	2.210	2.272	1.039	2.210	2.240	2.024	2.043
K	2.557	2.601	2.661	2.535	2.656	2.689	2.695	2.663
Na	2.215	2.320	2.516	2.282	2.504	2.492	2.432	2.366
ΣFe	2.134	2.492	2.425	2.285	3.104	2.774	2.788	2.633
Mn	3.149	3.636	3.668	3.347	3.762	3.727	3.477	3.591
Cu	5.502	5.502	5.502	5.803	5.502	5.372	6.201	5.573
Cd	5.574	6.051	5.750	5.750	5.750	5.619	6.051	5.574
Zn	2.935	3.225	3.368	3.030	3.324	3.271	3.067	3.099
Ni	3.354	3.810	3.924	3.565	3.905	3.866	3.601	3.686
Pb	9.000	9.000	9.000	9.000	9.000	9.000	9.000	9.000
Al	9.000	9.000	9.000	9.000	9.000	9.000	9.000	9.000
SO_4	1.369	1.569	1.406	1.343	1.614	1.625	1.426	1.445
$B(OH)_4$	3.571	3.691	3.672	3.478	3.712	3.779	3.587	3.654
MoO_4	9.000	9.000	9.000	9.000	9.000	9.000	9.000	9.000

Table A2. Lysimeter L610 Data Used in the GEOCHEM Evaluations (-log mol L^{-1}, unless noted otherwise) (continued)

Sample Number:	36L	40L	44L	48L	52L	54L	56L	60L
Elapsed Time, days:	963	982	1003	1024	1066	1129	1143	1171
pH (units)	3.25	3.58	3.45	3.48	3.13	2.98	3.06	2.96
pe (units)	5.75	5.42	5.55	5.52	5.87	6.02	5.94	6.04
Ca	1.895	2.047	2.035	2.084	2.035	1.959	1.980	1.940
Mg	2.043	2.130	2.307	2.499	2.272	2.130	2.155	2.107
K	2.778	2.760	2.836	2.920	2.803	2.743	2.638	2.690
Na	2.469	2.529	2.708	2.830	2.637	2.469	2.432	2.362
ΣFe	3.104	2.802	3.984	4.668	3.524	2.828	2.167	2.057
Mn	3.613	3.441	3.831	4.041	3.723	3.541	3.736	3.450
Cu	5.160	5.140	5.180	5.055	5.627	5.689	6.201	6.104
Cd	5.310	5.225	5.335	5.388	5.972	5.972	5.972	5.937
Zn	3.162	3.121	3.310	3.454	3.172	3.143	3.259	3.116
Ni	3.723	3.546	3.871	4.053	3.805	3.712	3.860	3.712
Pb	9.000	9.000	9.000	9.000	9.000	9.000	9.000	9.000
Al	9.000	9.000	2.285	2.390	2.390	2.592	2.586	2.798
SO_4	1.506	1.489	1.626	1.729	1.597	1.473	1.429	1.400
$B(OH)_4$	3.779	3.779	3.587	3.920	3.755	3.636	3.803	3.529
MoO_4	9.000	9.000	9.000	9.000	9.000	9.000	9.000	9.000

Table A2. Lysimeter L610 Data Used in the GEOCHEM Evaluations (-log mol L^{-1}, unless noted otherwise) (continued)

Sample Number:	62L	64L	68L	70L	6C	16C	26C	36C
Elapsed Time, days:	1234	1248	1283	1297	59	130	212	373
pH (units)	2.93	3.16	3.20	3.09	3.07	2.84	3.07	2.70
pe (units)	6.07	5.84	5.80	5.91	5.93	6.16	5.93	6.30
Ca	1.945	1.967	2.126	2.001	1.916	1.947	1.957	2.050
Mg	2.063	2.039	2.130	2.085	1.628	1.696	1.863	1.911
K	2.638	2.663	2.737	2.723	2.584	2.569	2.581	2.484
Na	2.362	2.453	2.549	2.759	1.925	1.935	2.109	2.228
ΣFe	2.007	2.069	2.543	2.551	1.690	2.219	2.437	2.309
Mn	3.384	3.461	3.710	3.616	2.992	3.106	3.072	3.322
Cu	6.201	5.900	5.441	5.599	6.025	5.849	5.762	6.326
Cd	6.051	5.875	5.604	5.636	5.218	4.954	5.005	5.200
Zn	3.125	3.182	3.324	3.192	2.491	2.744	2.444	2.824
Ni	3.756	3.844	3.943	3.782	3.036	3.225	3.169	3.189
Pb	9.000	9.000	9.000	9.000	5.886	5.584	5.714	4.918
Al	2.887	2.750	2.334	2.214	9.000	9.000	9.000	9.000
SO_4	1.369	1.408	1.542	1.452	1.093	1.165	1.402	1.314
$B(OH)_4$	3.515	3.542	3.755	3.733	3.206	3.242	3.413	3.593
MoO_4	9.000	9.000	9.000	9.000	5.369	5.903	5.137	4.903

Table A2. Lysimeter L610 Data Used in the GEOCHEM Evaluations (-log mol L^{-1}, unless noted otherwise) (continued)

Sample Number:	46C	56C	66C	76C	89C	96C	106C	116C
Elapsed Time, days:	415	456	505	540	610	680	736	771
pH (units)	2.92	2.54	3.26	2.65	2.86	2.95	3.10	3.06
pe (units)	6.08	6.46	5.74	6.35	6.14	6.05	5.90	5.94
Ca	1.893	1.994	1.946	1.983	1.969	1.904	1.969	1.980
Mg	1.789	1.819	1.922	2.020	1.988	1.842	1.881	1.923
K	2.459	2.544	2.659	2.673	2.753	2.592	2.621	2.506
Na	2.097	2.121	2.166	2.225	2.248	2.215	2.185	2.215
ΣFe	1.941	1.927	2.277	3.084	3.167	2.316	2.228	2.145
Mn	3.243	3.216	3.261	3.330	3.347	3.202	3.172	3.249
Cu	6.201	6.201	6.502	5.724	5.803	5.803	5.803	9.000
Cd	5.370	5.428	5.258	5.164	5.051	5.449	5.574	5.574
Zn	2.450	2.852	2.958	2.964	2.876	2.815	2.881	2.861
Ni	3.246	3.387	3.369	3.405	3.428	3.344	3.321	3.388
Pb	4.970	5.237	9.000	5.617	9.000	9.000	9.000	9.000
Al	9.000	9.000	9.000	9.000	9.000	9.000	9.000	9.000
SO_4	1.283	1.285	1.340	1.374	1.396	1.366	1.338	1.311
$B(OH)_4$	3.344	3.221	3.371	3.518	3.619	3.515	3.454	3.443
MoO_4	4.903	5.380	9.000	5.301	9.000	9.000	9.000	9.000

Table A2. Lysimeter L610 Data Used in the GEOCHEM Evaluations (-log mol L^{-1}, unless noted otherwise) (continued)

Sample Number:	126C	136C	146C	157C	166C	176C	186C	195C
Elapsed Time, days:	834	885	947	1003	1045	1115	1192	1269
pH (units)	3.19	3.81	3.66	3.85	3.37	3.21	2.94	3.27
pe (units)	5.81	5.19	5.34	5.15	5.63	5.79	6.06	5.73
Ca	1.990	1.950	1.871	1.969	1.990	1.950	1.940	2.001
Mg	2.005	2.043	1.881	2.063	2.130	2.085	2.063	2.005
K	2.588	2.539	2.636	2.753	2.773	2.758	2.712	2.623
Na	2.282	2.282	2.282	2.437	2.492	2.393	2.320	2.432
ΣFe	2.385	2.769	2.747	2.751	2.844	2.332	2.075	2.415
Mn	3.371	3.466	3.452	3.561	3.626	3.482	3.430	3.597
Cu	5.803	5.849	6.025	6.025	6.326	6.201	6.104	6.326
Cd	5.574	5.327	5.218	5.310	5.689	5.796	5.847	5.653
Zn	3.052	3.067	3.067	3.083	3.075	3.099	3.108	3.271
Ni	3.570	3.587	3.556	3.635	3.668	3.601	3.689	3.866
Pb	9.000	9.000	9.000	9.000	9.000	9.000	9.000	9.000
Al	9.000	9.000	9.000	2.227	2.176	2.317	2.477	2.301
SO_4	1.391	1.413	1.406	1.447	1.526	1.430	1.374	1.475
$B(OH)_4$	3.466	3.542	3.654	3.411	3.672	3.587	3.443	3.654
MoO_4	9.000	9.000	9.000	9.000	9.000	9.000	9.000	9.000

Table A2. Lysimeter L610 Data Used in the GEOCHEM Evaluations (-log mol L^{-1}, unless noted otherwise) (continued)

Sample Number:	3R	7R	11R	15R	19R	23R	27R	31R
Elapsed Time, days:	743	764	816	841	865	885	905	947
pH (units)	3.00	2.99	3.36	3.09	3.38	3.83	3.30	3.53
pe (units)	6.00	6.01	5.64	5.91	5.62	5.17	5.70	5.47
Ca	1.966	1.959	1.959	1.980	1.969	1.940	1.969	1.879
Mg	2.013	1.954	1.854	1.923	2.085	2.043	2.024	1.854
K	2.571	2.581	2.629	2.605	2.643	2.638	2.643	2.614
Na	2.301	2.248	2.185	2.215	2.407	2.320	2.422	2.282
ΣFe	2.264	2.203	2.405	2.385	2.934	2.706	3.251	2.833
Mn	3.263	3.277	3.235	3.235	3.544	3.477	3.480	3.418
Cu	5.502	5.803	5.803	5.803	5.803	5.627	6.025	5.803
Cd	5.449	5.449	5.574	5.449	5.449	5.398	5.905	5.280
Zn	3.067	2.861	2.970	2.958	3.153	3.083	3.075	3.067
Ni	3.442	3.407	3.420	3.416	3.697	3.619	3.601	3.549
Pb	9.000	9.000	9.000	9.000	9.000	9.000	9.000	9.000
Al	9.000	9.000	9.000	9.000	9.000	9.000	9.000	9.000
SO_4	1.407	1.325	1.424	1.292	1.425	1.413	1.378	1.360
$B(OH)_4$	3.454	3.411	3.400	3.400	3.542	3.529	3.542	3.654
MoO_4	9.000	9.000	9.000	9.000	9.000	9.000	9.000	9.000

Table A2. Lysimeter L610 Data Used in the GEOCHEM Evaluations (-log mol L^{-1}, unless noted otherwise) (continued)

Sample Number:	35R	39R	43R	47R	51R	55R	59R	63R
Elapsed Time, days:	975	991	1010	1038	1066	1087	1115	1143
pH (units)	3.40	3.51	3.53	3.61	3.31	3.43	3.33	2.97
pe (units)	5.60	5.49	5.47	5.39	5.69	5.57	5.67	6.03
Ca	1.959	1.990	1.967	1.969	1.980	1.969	1.950	1.940
Mg	2.085	1.988	2.089	2.043	2.043	2.155	2.085	2.085
K	2.735	2.753	2.769	2.766	2.729	2.713	2.687	2.662
Na	2.448	2.427	2.481	2.453	2.437	2.469	2.407	2.407
ΣFe	2.999	3.363	2.937	2.878	2.668	2.425	2.332	2.191
Mn	3.668	3.509	3.552	3.454	3.443	3.520	3.407	3.459
Cu	5.599	5.388	5.627	5.599	5.958	6.025	5.803	5.958
Cd	5.398	5.153	5.327	5.495	5.671	5.671	5.604	5.689
Zn	3.023	2.946	3.125	2.970	2.907	3.099	3.030	3.052
Ni	3.723	3.546	3.635	3.523	3.518	3.632	3.551	3.616
Pb	9.000	9.000	9.000	9.000	9.000	9.000	9.000	9.000
Al	9.000	9.000	2.164	2.000	2.109	2.285	2.255	2.352
SO_4	1.411	1.389	1.430	1.392	1.398	1.444	1.407	1.380
$B(OH)_4$	3.602	3.602	3.390	3.587	3.478	3.636	3.515	3.478
MoO_4	9.000	9.000	9.000	9.000	9.000	9.000	9.000	9.000

Table A2. Lysimeter L610 Data Used in the GEOCHEM Evaluations (-log mol L^{-1}, unless noted otherwise) (continued)

Sample Number:	67R	71R	75R	78R
Elapsed Time, days:	1171	1248	1268	1299
pH (units)	2.96	3.05	3.12	3.62
pe (units)	6.04	5.95	5.88	5.38
Ca	1.940	1.994	1.940	2.001
Mg	2.085	2.082	2.168	2.255
K	2.689	2.710	2.718	2.735
Na	2.362	2.407	2.549	2.759
ΣFe	2.039	2.137	2.969	2.902
Mn	3.422	3.397	3.705	3.800
Cu	6.104	5.849	5.223	5.212
Cd	5.905	5.796	5.407	5.546
Zn	3.091	3.116	3.297	3.384
Ni	3.629	3.716	3.871	3.956
Pb	9.000	9.000	9.000	9.000
Al	2.512	2.550	2.227	2.310
SO_4	1.369	1.378	1.494	1.577
$B(OH)_4$	3.490	3.502	3.712	3.858
MoO_4	9.000	9.000	9.000	9.000

Table A3. Lysimeter L710 Data Used in the GEOCHEM Evaluations (-log mol L^{-1}, unless noted otherwise)

Sample Number:	5L	15L	25L	35L	45L	55L	65L	75L
Elapsed Time, days:	66	136	243	289	359	429	498	582
pH (units)	2.94	2.94	2.68	2.67	2.61	2.48	2.84	2.63
pe (units)	6.06	6.06	6.32	6.33	6.39	6.52	6.16	6.37
Ca	2.225	1.926	2.086	2.005	2.006	1.976	2.010	2.012
Mg	0.995	1.026	1.491	1.416	1.458	1.616	1.671	1.687
K	5.362	4.449	4.171	4.302	4.260	3.868	3.714	3.918
Na	3.646	3.006	2.809	3.048	3.017	2.805	2.886	2.987
ΣFe	0.793	0.751	1.316	1.236	1.305	1.325	1.356	1.446
Mn	2.388	2.497	2.871	2.914	2.786	2.976	3.041	3.196
Cu	3.441	4.588	5.461	4.984	4.889	5.405	5.849	5.803
Cd	3.706	3.768	4.551	4.712	5.021	5.327	5.225	5.273
Zn	1.751	1.722	2.032	2.221	2.302	2.577	2.639	2.702
Ni	2.374	2.509	2.850	2.839	2.956	3.078	3.115	3.237
Pb	5.049	4.760	5.170	9.000	5.617	5.471	4.438	5.413
Al	9.000	9.000	2.107	2.047	2.224	2.723	2.913	2.768
SO_4	0.271	0.406	0.889	0.831	0.894	1.025	1.011	1.041
$B(OH)_4$	3.536	3.165	4.038	4.147	3.830	3.897	3.801	3.888
MoO_4	4.688	4.489	4.941	5.101	5.028	5.414	5.520	5.380

Table A3. Lysimeter L710 Data Used in the GEOCHEM Evaluations (-log mol L^{-1}, unless noted otherwise) (continued)

Sample Number:	85L	95L	105L	115L	125L	135L	145L	155L
Elapsed Time, days:	659	729	794	855	898	968	1010	1066
pH (units)	2.57	3.22	3.16	3.19	3.40	4.00	4.01	3.22
pe (units)	6.43	5.78	5.84	5.81	5.60	5.00	4.99	5.78
Ca	1.913	1.913	1.904	1.969	1.895	1.980	1.940	1.950
Mg	1.687	1.714	1.784	1.909	2.085	2.085	2.182	2.155
K	3.984	3.766	3.735	3.597	3.628	3.735	3.741	3.588
Na	2.805	2.749	2.516	2.856	2.759	3.000	3.106	3.116
ΣFe	1.446	1.446	1.446	1.601	1.765	1.783	1.908	1.849
Mn	3.059	3.117	3.221	3.378	3.564	3.536	3.661	3.626
Cu	5.803	9.000	9.000	9.000	9.000	9.000	6.326	9.000
Cd	5.449	5.750	5.574	5.574	6.352	6.449	5.796	6.097
Zn	2.611	2.774	2.958	3.338	3.669	3.736	3.736	4.037
Ni	3.200	3.263	3.337	3.565	3.814	3.814	3.990	3.924
Pb	9.000	9.000	9.000	9.000	9.000	9.000	9.000	9.000
Al	3.000	3.477	3.954	4.431	4.431	4.130	4.431	9.000
SO_4	1.112	1.181	1.172	1.252	1.389	1.449	1.489	1.437
$B(OH)_4$	4.034	3.992	3.830	3.830	4.034	4.131	3.955	4.034
MoO_4	9.000	9.000	9.000	9.000	9.000	9.000	9.000	9.000

Table A3. Lysimeter L710 Data Used in the GEOCHEM Evaluations (-log mol L^{-1}, unless noted otherwise) (continued)

Sample Number:	165L	175L	185L	189L	7C	16C	25C	34C
Elapsed Time, days:	1129	1199	1269	1299	66	164	250	303
pH (units)	3.46	2.98	3.05	3.90	2.57	2.60	2.41	2.51
pe (units)	5.54	6.02	5.95	5.10	6.43	6.40	6.59	6.49
Ca	1.931	1.922	1.922	1.935	1.934	1.993	2.064	2.030
Mg	2.272	2.182	2.130	2.307	0.865	0.986	1.109	1.145
K	3.605	3.485	3.482	3.462	5.416	5.230	5.270	5.212
Na	2.805	2.981	2.964	3.061	3.856	3.234	3.203	3.384
ΣFe	1.866	1.866	1.908	1.955	0.862	0.803	1.039	1.103
Mn	3.626	3.626	3.740	3.837	2.386	2.475	2.597	2.619
Cu	9.000	6.502	6.201	6.803	2.946	3.917	4.267	4.258
Cd	5.937	6.097	6.273	6.574	3.691	3.872	4.092	4.193
Zn	4.213	4.213	4.338	4.815	1.688	2.076	1.654	1.926
Ni	4.070	4.167	4.769	4.769	2.430	2.430	2.570	2.562
Pb	9.000	9.000	9.000	9.000	5.015	5.112	9.000	9.000
Al	9.000	4.653	4.431	9.000	9.000	1.390	1.590	1.674
SO_4	1.441	1.424	1.476	1.553	0.203	0.352	0.503	0.617
$B(OH)_4$	3.992	3.992	4.131	4.335	3.682	3.594	4.286	4.270
MoO_4	9.000	9.000	9.000	9.000	4.277	4.703	9.000	5.018

Table A3. Lysimeter L710 Data Used in the GEOCHEM Evaluations (-log mol L^{-1}, unless noted otherwise) (continued)

Sample Number:	43C	52C	61C	70C	79C	88C	97C	106C
Elapsed Time, days:	380	442	512	610	680	743	799	855
pH (units)	2.43	2.19	2.44	2.36	2.52	2.57	2.35	2.64
pe (units)	6.57	6.81	6.56	6.64	6.48	6.43	6.65	6.36
Ca	1.957	1.990	1.967	2.023	2.012	1.938	1.839	2.001
Mg	1.190	1.329	1.479	1.580	1.600	1.599	1.687	1.723
K	5.012	4.313	4.181	3.969	4.225	4.177	4.349	4.108
Na	3.188	2.955	2.950	3.041	2.981	2.817	2.583	2.930
ΣFe	1.112	1.221	1.242	1.349	1.468	1.471	1.543	1.583
Mn	2.594	2.695	2.969	3.000	2.927	2.947	3.127	3.196
Cu	4.434	4.573	4.731	5.025	5.025	4.812	5.104	5.025
Cd	4.479	4.866	5.176	5.009	5.273	5.206	5.449	5.449
Zn	1.995	2.247	2.437	2.560	2.585	2.663	2.715	2.838
Ni	2.651	2.769	2.962	3.070	3.044	3.321	3.225	3.292
Pb	9.00	5.275	5.617	5.316	9.000	9.000	9.000	9.000
Al	9.000	2.157	2.528	2.723	2.699	2.875	3.033	3.051
SO_4	0.724	0.793	0.861	0.992	1.038	1.055	1.121	1.127
$B(OH)_4$	4.142	3.973	3.888	3.920	4.131	3.992	3.955	3.888
MoO_4	9.000	5.137	5.640	5.380	9.000	9.000	9.000	9.000

Table A3. Lysimeter L710 Data Used in the GEOCHEM Evaluations (-log mol L^{-1}, unless noted otherwise) (continued)

Sample Number:	115C	124C	133C	142C	151C	160C	169C	178C
Elapsed Time, days:	892	954	996	1038	1094	1157	1213	1297
pH (units)	2.95	2.96	3.07	3.03	3.07	2.88	2.46	2.76
pe (units)	6.05	6.04	5.93	5.97	5.93	6.12	6.54	6.24
Ca	1.990	2.001	1.958	1.980	1.980	1.863	1.969	1.926
Mg	1.923	1.909	1.950	1.971	2.043	2.005	1.966	2.043
K	3.673	3.753	3.747	3.700	3.584	3.513	3.584	3.847
Na	2.947	2.981	2.992	3.131	3.046	2.549	2.930	3.061
ΣFe	1.633	1.633	1.664	1.706	1.706	1.633	1.751	1.706
Mn	3.325	3.325	3.457	3.463	3.463	3.439	3.430	3.610
Cu	5.573	5.724	5.900	6.502	6.326	6.502	6.326	9.000
Cd	5.407	5.671	5.636	5.937	5.559	5.619	5.937	6.097
Zn	3.116	3.037	3.324	3.418	3.669	3.774	3.815	4.213
Ni	3.509	3.458	3.593	3.651	3.716	3.735	3.752	4.115
Pb	9.000	9.000	9.000	9.000	9.000	9.000	9.000	9.000
Al	3.586	3.528	3.829	3.954	4.431	4.829	4.477	9.000
SO_4	1.272	1.239	1.302	1.366	1.338	1.343	1.273	1.335
$B(OH)_4$	4.034	3.955	4.034	4.034	4.034	3.888	3.888	4.131
MoO_4	9.000	9.000	9.000	9.000	9.000	9.000	9.000	9.000

Table A3. Lysimeter L710 Data Used in the GEOCHEM Evaluations (-log mol L^{-1}, unless noted otherwise) (continued)

Sample Number:	7R	16R	25R	34R	43R	52R	61R	70R
Elapsed Time, days:	80	164	250	303	373	435	505	582
pH (units)	3.04	2.89	2.41	2.72	2.55	2.57	2.88	2.51
pe (units)	5.96	6.11	6.59	6.28	6.45	6.43	6.12	6.49
Ca	1.905	1.987	2.087	2.004	1.987	2.009	1.977	1.734
Mg	0.954	0.907	1.166	1.233	1.171	1.369	1.386	1.240
K	5.478	4.468	4.337	4.465	4.061	3.844	3.719	3.885
Na	3.268	2.981	3.061	3.152	3.054	2.850	2.805	2.983
ΣFe	0.786	0.714	1.090	1.107	1.074	1.204	1.179	1.057
Mn	2.517	2.291	2.661	2.723	2.679	2.710	2.920	2.749
Cu	3.259	4.459	5.573	5.170	5.247	5.573	5.958	9.000
Cd	3.752	3.671	4.335	4.392	4.745	5.111	5.417	5.051
Zn	1.766	1.935	1.695	1.995	2.009	2.276	2.340	2.203
Ni	2.488	2.198	2.619	2.629	2.699	2.796	2.899	3.115
Pb	4.811	4.693	9.000	9.000	9.000	5.362	5.839	5.275
Al	9.000	1.363	9.000	1.819	9.000	2.227	2.497	2.683
SO_4	0.279	0.275	0.539	0.675	0.681	0.806	0.835	0.929
$B(OH)_4$	3.695	3.590	4.636	4.115	3.930	3.830	3.691	3.830
MoO_4	4.265	4.301	9.000	4.871	9.000	5.226	5.551	5.137

Table A3. Lysimeter L710 Data Used in the GEOCHEM Evaluations (-log mol L^{-1}, unless noted otherwise) (continued)

Sample Number:	79R	88R	97R	106R	115R	124R	133R	142R
Elapsed Time, days:	652	715	771	827	876	926	977	1017
pH (units)	2.57	2.80	2.85	2.97	3.03	3.20	3.43	3.18
pe (units)	6.43	6.20	6.15	6.03	5.97	5.80	5.57	5.82
Ca	2.012	1.925	1.904	1.990	2.001	1.950	1.959	1.990
Mg	1.638	1.633	1.687	1.773	1.939	1.867	2.063	2.085
K	3.821	3.810	3.796	3.663	3.592	3.592	3.678	3.633
Na	2.738	2.820	2.805	2.884	2.947	2.856	3.000	3.085
ΣFe	1.446	1.419	1.425	1.501	1.668	1.601	1.783	1.828
Mn	3.208	2.984	3.087	3.106	3.325	3.418	3.397	3.564
Cu	9.000	6.104	9.000	9.000	9.000	9.000	6.803	6.803
Cd	5.574	5.352	6.051	5.352	5.574	5.559	5.729	5.729
Zn	2.669	2.622	2.774	2.815	3.030	3.116	3.353	3.514
Ni	3.212	3.125	3.087	3.250	3.490	3.513	3.565	3.727
Pb	9.000	9.000	9.000	9.000	9.000	9.000	9.000	9.000
Al	2.818	2.875	3.227	3.390	3.586	3.732	3.829	3.954
SO_4	1.047	1.085	1.158	1.148	1.226	1.255	1.394	1.448
$B(OH)_4$	3.992	3.888	3.733	3.672	3.830	3.888	3.955	3.691
MoO_4	5.204	9.000	9.000	9.000	9.000	9.000	9.000	9.000

Table A3. Lysimeter L710 Data Used in the GEOCHEM Evaluations (-log mol L^{-1}, unless noted otherwise) (continued)

Sample Number:	151R	160R	169R	178R
Elapsed Time, days:	1073	1129	1192	1255
pH (units)	3.16	3.11	2.78	2.35
pe (units)	5.84	5.89	6.22	6.65
Ca	1.922	1.959	1.931	1.964
Mg	2.043	2.107	2.085	1.920
K	3.555	3.465	3.437	3.895
Na	3.069	2.830	2.899	2.843
ΣFe	1.779	1.769	1.884	1.896
Mn	3.509	3.509	3.509	3.418
Cu	6.803	9.000	6.803	6.104
Cd	5.905	5.796	6.051	6.148
Zn	3.611	3.912	4.116	3.861
Ni	3.655	3.727	3.769	3.814
Pb	9.000	9.000	9.000	9.000
Al	4.130	9.000	3.954	3.954
SO_4	1.403	1.373	1.387	1.302
$B(OH)_4$	3.920	3.888	3.779	3.888
MoO_4	9.000	9.000	9.000	9.000

APPENDIX B

Reactions and Equilibrium Constants Used in the Geochemical Model Evaluations

Table B1. Aqueous Phase Chemical Reactions and Equilibrium Constants Used by GEOCHEM

Reaction	Log K
$Ca^{2+} + SO_4^{2-} = CaSO_4^0$	2.3
$Ca^{2+} + B(OH)_4^- = CaB(OH)_4^+$	1.8
$Ca^{2+} + MoO_4^{2-} = CaMoO_4^0$	3.1
$Ca^{2+} + H_2O = CaOH^+ + H^+$	-12.6
$Mg^{2+} + SO_4^{2-} = MgSO_4^0$	2.2
$Mg^{2+} + B(OH)_4^- = MgB(OH)_4^+$	1.6
$Mg^{2+} + MoO_4^{2-} = MgMoO_4^0$	3.7
$Mg^{2+} + H_2O = MgOH^+ + H^+$	-11.8
$4Mg^{2+} + 4H_2O = Mg_4(OH)_4^{4+} + 4H^+$	-39.7
$K^+ + SO_4^{2-} = KSO_4^-$	0.9
$K^+ + H^+ + SO_4^{2-} = KHSO_4^0$	1.9
$2K^+ + SO_4^{2-} = K_2SO_4^0$	1.5
$K^+ + MoO_4^{2-} = KMoO_4^-$	1.3
$K^+ + B(OH)_4^- = KB(OH)_4^0$	0.0
$K^+ + H_2O = KOH^0 + H^+$	-14.5
$Na^+ + SO_4^{2-} = NaSO_4^-$	1.1
$Na^+ + H^+ + SO_4^{2-} = NaHSO_4^0$	2.0
$2Na^+ + SO_4^{2-} = Na_2SO_4^0$	1.5
$Na^+ + MoO_4^{2-} = NaMoO_4^-$	1.7
$Na^+ + B(OH)_4^- = NaB(OH)_4^0$	0.3
$Na^+ + H_2O = NaOH^0 + H^+$	-14.2

Table B1. Aqueous Phase Chemical Reactions and Equilibrium Constants Used by GEOCHEM (continued)

Reaction	Log K
$Fe^{3+} + SO_4^{2-} = FeSO_4^{+}$	4.0
$Fe^{3+} + 2SO_4^{2-} = Fe(SO_4)_2^{-}$	5.4
$Fe^{3+} + 3SO_4^{2-} = Fe(SO_4)_3^{3-}$	4.0
$Fe^{3+} + H^{+} + SO_4^{2-} = FeHSO_4^{2+}$	4.5
$Fe^{3+} + B(OH)_4^{-} = FeB(OH)_4^{2+}$	8.9
$Fe^{3+} + 2B(OH)_4^{-} = Fe(B(OH)_4)_2^{+}$	15.8
$Fe^{3+} + H_2O = FeOH^{2+} + H^{+}$	-2.2
$Fe^{3+} + 2H_2O = Fe(OH)_2^{+} + 2H^{+}$	-5.7
$Fe^{3+} + 3H_2O = Fe(OH)_3^{0} + 3H^{+}$	-12.0
$Fe^{3+} + 4H_2O = Fe(OH)_4^{-} + 4H^{+}$	-21.6
$2Fe^{3+} + 2H_2O = Fe_2(OH)_2^{4+} + 2H^{+}$	-3.0
$3Fe^{3+} + 4H_2O = Fe_3(OH)_4^{5+} + 4H^{+}$	-6.3
$Fe^{3+} + e^{-} = Fe^{2+}$	13.0
$Fe^{2+} + SO_4^{2-} = FeSO_4^{0}$	2.2
$Fe^{2+} + 2SO_4^{2-} = Fe(SO_4)_2^{2-}$	0.8
$Fe^{2+} + 3SO_4^{2-} = Fe(SO_4)_3^{4-}$	-4.3
$Fe^{2+} + H^{+} + SO_4^{2-} = FeHSO_4^{+}$	3.0
$Fe^{2+} + B(OH)_4^{-} = FeB(OH)_4^{+}$	3.9
$Fe^{2+} + H_2O = FeOH^{+} + H^{+}$	-9.5
$Fe^{2+} + 2H_2O = Fe(OH)_2^{0} + 2H^{+}$	-20.6
$Fe^{2+} + 3H_2O = Fe(OH)_3^{-} + 3H^{+}$	-31.0
$Fe^{2+} + 4H_2O = Fe(OH)_4^{2-} + 4H^{+}$	-46.0

Table B1. Aqueous Phase Chemical Reactions and Equilibrium Constants Used by GEOCHEM (continued)

Reaction	Log K
$Mn^{2+} + SO_4^{2-} = MnSO_4^0$	2.3
$Mn^{2+} + 2SO_4^{2-} = Mn(SO_4)_2^{2-}$	0.9
$Mn^{2+} + 3SO_4^{2-} = Mn(SO_4)_3^{4-}$	-4.1
$Mn^{2+} + H^+ + SO_4^{2-} = MnHSO_4^+$	2.9
$Mn^{2+} + B(OH)_4^- = MnB(OH)_4^+$	4.9
$Mn^{2+} + H_2O = MnOH^+ + H^+$	-10.6
$Mn^{2+} + 2H_2O = Mn(OH)_2^0 + 2H^+$	-22.2
$Mn^{2+} + 3H_2O = Mn(OH)_3^- + 3H^+$	-34.8
$Mn^{2+} + 4H_2O = Mn(OH)_4^{2-} + 4H^+$	-48.3
$2Mn^{2+} + 3H_2O = Mn_2(OH)_3^+ + 3H^+$	-23.9
$Cu^{2+} + SO_4^{2-} = CuSO_4^0$	2.4
$Cu^{2+} + 2SO_4^{2-} = Cu(SO_4)_2^{2-}$	1.1
$Cu^{2+} + 3SO_4^{2-} = Cu(SO_4)_3^{4-}$	-3.9
$Cu^{2+} + H^+ + SO_4^{2-} = CuHSO_4^+$	3.0
$Cu^{2+} + B(OH)_4^- = CuB(OH)_4^+$	4.5
$Cu^{2+} + 2B(OH)_4^- = Cu(B(OH)_4)_2^0$	5.9
$Cu^{2+} + H_2O = CuOH^+ + H^+$	-8.0
$Cu^{2+} + 2H_2O = Cu(OH)_2^0 + 2H^+$	-17.3
$Cu^{2+} + 3H_2O = Cu(OH)_3^- + 3H^+$	-27.8
$Cu^{2+} + 4H_2O = Cu(OH)_4^{2-} + 4H^+$	-39.6
$2Cu^{2+} + 2H_2O = Cu_2(OH)_2^{2+} + 2H^+$	-10.4

Table B1. Aqueous Phase Chemical Reactions and Equilibrium Constants Used by GEOCHEM (continued)

Reaction	Log K
$Cd^{2+} + SO_4^{2-} = CdSO_4^0$	2.5
$Cd^{2+} + 2SO_4^{2-} = Cd(SO_4)_2^{2-}$	2.9
$Cd^{2+} + 3SO_4^{2-} = Cd(SO_4)_3^{4-}$	1.9
$Cd^{2+} + H^+ + SO_4^{2-} = CdHSO_4^+$	2.9
$Cd^{2+} + B(OH)_4^- = CdB(OH)_4^+$	3.7
$Cd^{2+} + 4B(OH)_4^- = Cd(B(OH)_4)_4^{2-}$	10.6
$Cd^{2+} + H_2O = CdOH^+ + H^+$	-10.1
$Cd^{2+} + 2H_2O = Cd(OH)_2^0 + 2H^+$	-20.4
$Cd^{2+} + 3H_2O = Cd(OH)_3^- + 3H^+$	-33.3
$Cd^{2+} + 4H_2O = Cd(OH)_4^{2-} + 4H^+$	-47.4
$4Cd^{2+} + 4H_2O = Cd_4(OH)_4^{4+} + 4H^+$	-32.9
$Zn^{2+} + SO_4^{2-} = ZnSO_4^0$	2.4
$Zn^{2+} + 2SO_4^{2-} = Zn(SO_4)_2^{2-}$	1.1
$Zn^{2+} + 3SO_4^{2-} = Zn(SO_4)_3^{4-}$	-3.8
$Zn^{2+} + H^+ + SO_4^{2-} = ZnHSO_4^+$	3.0
$Zn^{2+} + B(OH)_4^- = ZnB(OH)_4^+$	4.0
$Zn^{2+} +4B(OH)_4^- = Zn(B(OH)_4)_4^{2-}$	11.8
$Zn^{2+} + H_2O = ZnOH^+ + H^+$	-9.0
$Zn^{2+} + 2H_2O = Zn(OH)_2^0 + 2H^+$	-16.9
$Zn^{2+} + 3H_2O = Zn(OH)_3^- + 3H^+$	-28.4
$Zn^{2+} + 4H_2O = Zn(OH)_4^{2-} + 4H^+$	-41.2
$2Zn^{2+} + 6H_2O = Zn_2(OH)_6^{2-} + 6H^+$	-57.8

Table B1. Aqueous Phase Chemical Reactions and Equilibrium Constants Used by GEOCHEM (continued)

Reaction	Log K
$Ni^{2+} + SO_4^{2-} = NiSO_4^0$	2.3
$Ni^{2+} + 2SO_4^{2-} = Ni(SO_4)_2^{2-}$	1.0
$Ni^{2+} + 3SO_4^{2-} = Ni(SO_4)_3^{4-}$	-3.9
$Ni^{2+} + H^+ + SO_4^{2-} = NiHSO_4^+$	3.0
$Ni^{2+} + B(OH)_4^- = NiB(OH)_4^+$	4.4
$Ni^{2+} + 3B(OH)_4^- = Ni[B(OH)_4]_3^-$	8.4
$Ni^{2+} + H_2O = NiOH^+ + H^+$	-9.9
$Ni^{2+} + 2H_2O = Ni(OH)_2^0 + 2H^+$	-19.0
$Ni^{2+} + 3H_2O = Ni(OH)_3^- + 3H^+$	-30.0
$Ni^{2+} + 4H_2O = Ni(OH)_4^{2-} + 4H^+$	-44.0
$4Ni^{2+} + 4H_2O = Ni_4(OH)_4^{4+} + 4H^+$	-27.7
$Pb^{2+} + SO_4^{2-} = PbSO_4^0$	2.6
$Pb^{2+} + 2SO_4^{2-} = Pb(SO_4)_2^{2-}$	3.5
$Pb^{2+} + 3SO_4^{2-} = Pb(SO_4)_3^{4-}$	2.6
$Pb^{2+} + H^+ + SO_4^{2-} = PbHSO_4^+$	2.8
$Pb^{2+} + B(OH)_4^- = PbB(OH)_4^+$	5.2
$Pb^{2+} + 2B(OH)_4^- = Pb(B(OH)_4)_2^0$	11.1
$Pb^{2+} + 3B(OH)_4^- = Pb(B(OH)_4)_3^-$	11.2
$Pb^{2+} + H_2O = PbOH^+ + H_2O$	-7.7
$Pb^{2+} + 2H_2O = Pb(OH)_2^0 + 2H_2O$	-17.1
$Pb^{2+} + 3H_2O = Pb(OH)_3^- + 3H_2O$	-28.1
$Pb^{2+} + 4H_2O = Pb(OH)_4^{2-} + 4H_2O$	-39.7
$4Pb^{2+} + 4H_2O = Pb_4(OH)_4^{4+} + 4H_2O$	-23.9

Table B1. Aqueous Phase Chemical Reactions and Equilibrium Constants Used by GEOCHEM (continued)

Reaction	Log K
$Al^{3+} + SO_4^{2-} = AlSO_4^+$	3.2
$Al^{3+} + 2SO_4^{2-} = Al(SO_4)_2^-$	1.9
$Al^{3+} + 3SO_4^{2-} = Al(SO_4)_3^{3-}$	-1.9
$Al^{3+} + B(OH)_4^- = AlB(OH)_4^{2+}$	7.6
$Al^{3+} + 2B(OH)_4^- = Al(B(OH)_4)_2^+$	14.6
$Al^{3+} + 3B(OH)_4^- = Al(B(OH)_4)_3^0$	20.0
$Al^{3+} + 6B(OH)_4^- = Al(B(OH)_4)_6^{3-}$	38.5
$Al^{3+} + H_2O = AlOH^{2+} + H^+$	-5.0
$Al^{3+} + 2H_2O = Al(OH)_2^+ + 2H^+$	-9.3
$Al^{3+} + 3H_2O = Al(OH)_3^0 + 3H^+$	-15.0
$Al^{3+} + 4H_2O = Al(OH)_4^- + 4H^+$	-22.1
$2Al^{3+} + 2H_2O = Al_2(OH)_2^{4+} + 2H^+$	-7.7
$3Al^{3+} + 4H_2O = Al_3(OH)_4^{5+} + 4H^+$	-13.9
$H^+ + SO_4^{2-} = HSO_4^-$	2.0
$2H^+ + SO_4^{2-} = H_2SO_4^0$	-8.3
$H^+ + B(OH)_4^- = B(OH)_3^0 + H_2O$	9.2
$H^+ + MoO_4^{2-} = HMoO_4^-$	4.2
$2H^+ + MoO_4^{2-} = H_2MoO_4^0$	8.2
$3H^+ + MoO_4^{2-} = MoO_2(OH)^+ + H_2O$	8.2
$4H^+ + MoO_4^{2-} = MoO_2 + 2H_2O$	8.6